



3 1176 00156 5572

NASA TM - 80135

NASA Technical Memorandum 80135

NASA-TM-80135 19790023882

ACOUSTICAL PROPERTIES OF HIGHLY POROUS FIBROUS MATERIALS

FOR REFERENCE

NOT TO BE TAKEN FROM THIS ROOM

ROBERT F. LAMBERT

JULY 1979

LIBRARY COPY

AUG 10 1979

LANGLEY RESEARCH CENTER
LIBRARY, NASA
HAMPTON, VIRGINIA

NASA

National Aeronautics and
Space Administration

Langley Research Center
Hampton, Virginia 23665

LIST OF SYMBOLS

A	$\text{Im} \left(\frac{\omega}{c_a} \Gamma_a \right)$ normalized attenuation constant
B	$\text{Re} \left(\frac{\omega}{c_a} \Gamma_a \right)$ normalized phase constant
c_a	speed of sound in the air of the pores
c_e	effective speed of sound in the air of the pores (see Appendix)
c_s	speed of compressional waves in the frame structure
c_o	speed of sound in air in free space
d	mean diameter of a filament in fibrous structure
i	$\sqrt{-1}$
k	$k_s / \kappa_a P_o \gamma$, generalized structure factor
k_s	structure factor for air in the pores
l	depth of sample of finite size
p	instantaneous acoustic pressure in the air of the pores
P_o	static acoustic pressure in the air of the pores
P_a	acoustic pressure amplitude in the air of the pores
P_s	acoustic pressure amplitude in the porous frame structure
Q	$\omega \rho / \Phi$, generalized acoustic quality factor
S	$\omega \rho + i \Phi$, generalized particle velocity coupling coefficient
V_a	acoustic particle velocity amplitude in the air of the pores
V_s	acoustic particle velocity amplitude in the porous frame structure
Y_a	complex acoustic admittance of air in the pores
Y_s	complex acoustic admittance of the porous frame structure
Z_a	complex acoustic impedance of the air in the pores
Z_s	complex acoustic impedance of the porous frame structure

N79-32053 #

LIST OF SYMBOLS

α	attenuation constant
α_a	normal incidence intensity absorption coefficient
β	phase constant
δ	instantaneous acoustic density ratio
γ	1.4, ratio of the specific heats for air
Γ	complex propagation constant
Γ_a	complex propagation constant for sound waves in the air of the pores
Γ_s	complex propagation constant for sound waves in the elastic frame structure
κ_a	bulk modulus for air in the pores
κ_s	bulk modulus for elastic frame material
κ	generalized dilatational coupling coefficient
ρ_a	apparent density of air in the pores at high frequencies
ρ_e	effective density of air in the pores at all frequencies (see Appendix)
ρ_{ei}	$\rho_0(k_s - 1)/\Omega$, effective density in the inertial coupling coefficient
ρ_{es}	effective density of the frame structure
ρ_0	mean density of air in free space
ρ_s	mean density of the material of the frame structure
ν	coefficient of kinematic viscosity for air
Φ	specific flow resistance of air in the pores
Φ_e	dynamic resistance of the air in the pores (see Appendix)
σ	generalized elastic coupling coefficient
Ω	porosity of the frame structure
ω	angular frequency of excitation

I. Introduction

Highly porous, fibrous materials play an important role in the technology of sound control. Such materials are used in a wide variety of forms and configurations for special purposes. Some fibrous materials such as glass fibers are synthetic and are spun together to form a flexible blanket while others appear as open-cell elastic foams. Others consist of natural fibers such as wool or hair felt. Most are available in a range of porosities and densities. Natural surfaces such as ground cover sometimes are modelled analytically, somewhat similar to fibrous bulk materials. Frequently, the bulk material is covered by a facing to prevent damage, provide mechanical support, and even change appearance.

Interest in this study is confined to acoustical properties of bulk materials and how their physical parameters influence acoustical characteristics such as normal incidence impedance and intensity absorption coefficient at its surface. No attempt is made to optimize performance in a particular application. In spite of the widespread application of both commercial and natural fibrous materials and their importance in noise control very little basic research has been conducted since the pioneering work of Scott⁽¹⁾, Zwicker and Kosten⁽²⁾, Morse and Bolt⁽³⁾, Beranek⁽⁴⁾ and R. W. Morse⁽⁵⁾ to mention a few early workers. Their primary motivation was better understanding in applications to architectural acoustics.

In this report the properties of fibrous materials (blanket, foam, and stiff tile) are formulated analytically on the basis of the theory of Zwicker and Kosten⁽²⁾ as applied to elastic frames. So, fundamentally, the equations

of motion are not new. However, they are recast into a form that identifies and hopefully clarifies certain aspects of coupling between sound waves in the air of the pore space and compressional elastic waves in the fibrous frame structure. Analytical solutions are then obtained for weak coupling, which appears to be most valid for highly porous materials, and an attempt is made to specify the minimum number of acoustical parameters required to characterize the behavior, and to establish any apparent frequency limitations in the characterization. The ultimate objective is to develop design procedures required in critical applications such as flow duct acoustics.

The coupled mode theory of Zwikker and Kosten sometimes has been criticized as being somewhat ad-hoc and too complicated. While this may be true for certain simple applications it is not valid for critical design where specific impedance values are needed. One important reason for studying coupled wave motion in bulk elastic materials is a better understanding of the behavior of duct liner surfaces that may exhibit extended reaction. Flexible fibrous materials that exhibit weak coupling are not likely to be locally reacting especially if the sound speed in the air of the pore space is much different from that of the sound speed of the incident wave.

Several experimental studies were carried out in an impedance tube to establish properties of small samples of a highly porous, fibrous material called Kevlar 29. One type had been studied earlier and some of its bulk properties were known⁽⁶⁾. Kevlar 29 consists of long, very fine fibers, and has excellent sound absorptive properties in bulk form⁽⁷⁾. There are two types, one in which the fibers are layered and the other in which the fibers are woven to form a more dense and stiffer blanket. These absorptive properties have been ascribed⁽⁷⁾ to a very slow phase speed at low frequencies which leads to

short wavelengths and more wavelengths per unit depth of sample. The attenuation at very low frequencies is about 2π nepers per wavelength. In this report experimental values of normal incidence impedance and absorption coefficient are compared with predictions based on decoupled wave motion. The agreement with theory is satisfactory if the so-called structure factor (ratio of apparent density of air in the pores to the mean density of air in free space) is adjusted to provide a good fit to impedance data. A parametric procedure was established to provide that fit. Future work could concentrate on a characterization based on coupled wave motion if low frequency impedance data (below 300 Hz) becomes available. The weak coupling formulas are derived in this report.

A comprehensive experimental study had been conducted earlier on the acoustical properties of a highly porous, open-cell, flexible, fibrous foam called Scottfoam⁽⁸⁾. This material also has excellent absorptive properties and a comparable parametric study yielded satisfactory results based on decoupled motion. It turned out that an acoustical quality factor index for Scottfoam was roughly twice that for Kevlar which makes it a very efficient bulk absorber. Microscopic study revealed that the filaments in the cellular structure have a mean diameter comparable with that of Kevlar, see Table I.

In the section on parametric studies an initial attempt is made to relate some of the material parameters in the theory of Zwikker and Kosten to parameters developed by others notably Morse⁽⁵⁾ and Hersh and Walker⁽⁷⁾. Also, in the appendix a new derivation of the equivalent density and dynamic resistance for porous materials as first proposed by Beranek⁽⁴⁾ is presented. While not directly relevant to this paper it could have considerable relevance if future work on the extended reaction of bulk materials in duct liners is

undertaken. It turns out that these more specialized theories can be brought into agreement with the theory of Zwicker and Kosten by suitable definitions.

In the following section a reformulation of the equations of motion and resulting characteristic equation based on the theory of Zwicker and Kosten is presented and discussed. The notation is consistent with that used in a modern textbook such as Morse and Ingard⁽⁹⁾.

Use of commercial products or names of manufacturers in this report does not constitute official endorsement of such products or manufacturers, either expressed or implied, by the National Aeronautics and Space Administration.

II. Analysis

A. Characteristic Equation

One of the important questions raised in the introduction is deciding whether or not sound waves in the pore space and elastic waves in the fibrous frame are coupled in any significant way. Roughly speaking one expects maximum coupling to occur when the phase velocity of sound waves in the air is equal to that of the longitudinal elastic waves in the frame. This coupling is both inertial and dissipational and is caused by differences in the wave particle velocities which must be accounted for in the balance of forces. Also present is coupling due to different pressure forces which act on the volume under consideration and produce changes in volume which are expressed in terms of "elastic constants" in the gas and in the frame of fibers. This coupling must be accounted for in the equations of continuity which conserves the total mass in a given volume of material. The elastic constant of the gas is fairly well defined but the elastic constant of the frame is not so well defined and hence not easily measureable either. Usually a static value is used^(2,4). At present this matter can only be resolved by doing careful measurements with the objective of resolving any discrepancies between measured and predicted values of the propagation constants, surface impedance, and acoustical absorption properties based on decoupled motion. Therefore, it is worthwhile studying wave coupling for the case of flexible, highly porous materials consisting of fine fibers and determining what physical properties are required to effectively decouple the motion especially in the lower ranges of frequencies say below 500 Hz. Since the air motion is viscous controlled over a fairly wide range of frequencies for such materials it is not immediately obvious as to exactly what requirements must be satisfied.

Thick samples of porous materials are homogeneous for all practical purposes and by considering plane wave propagation in one given direction the material may be considered isotropic. However, some fibrous materials are layered causing the material to be anisotropic. Thus any angular dependence of either impedance or absorption coefficient could not easily be inferred from either normal incidence measurements or a one-dimensional theory. Foam materials on the other hand, appear isotropic with no preferred orientation of the intercommunicating filaments and hence are probably easier to analyze and project results.

It was decided to use the basic formulation due to Zwikker and Kosten as a starting point in the analysis but to recast the notation in a more familiar form and use definitions as presented in a modern text like Morse and Ingard⁽⁹⁾. Following linear theory the relationship between the changes in air density δ caused by acoustic pressure disturbance p in the pore space is assumed to be of the form

$$\delta = \rho_0 \kappa_a p \quad (1)$$

where ρ_0 is the mean density of the air and κ_a is the bulk modulus of the air which, generally speaking, is frequency dependent. For very low frequencies and very fine pores it is assumed to take on its isothermal value

$1/P_0$ where P_0 is the static pressure while at sufficiently high frequencies it is assumed adiabatic, i.e. $\kappa_a = 1/P_0 \gamma$ where γ is the ratio of specific heats for air. Initially no assumption about the value of κ_a will be made except that it is treated as a real number. That matter can be deferred to a parametric analysis, Section III.

The solid frame structure of the porous material is characterized in vacuum by a bulk modulus κ_s and a mean mass density ρ_s in a manner similar to that of air. This type of elastic medium supports shear waves but only internal coupling effects of compressional waves is important for normal incidence predictions. The dependence of κ_s on frequency is not known, generally speaking, for most fibrous porous materials including foams. Initially no assumption about κ_s will be made either.

Another parameter of great importance is the "apparent density" of the air in the pores, ρ_a . Some fibers will move with the air as sound propagates thereby increasing its apparent density. Also, the air particle motion is constrained by the presence of constrictions and the apparent density is increased when air is forced to move through such constrictions. At sufficiently high frequencies the density of the air in the pores is assumed to be given by⁽²⁾

$$\rho_a = \rho_0 \frac{k_s}{\Omega} \quad (2)$$

where k_s is called a "structure factor" which supposedly accounts for the increase in air density caused by constrictions and blind passages, and

Ω is the porosity of the bulk material. Note, an increase in density caused by motion of the fibers is not included in ρ_a .

That matter is accounted for in a different way, see appendix A. For most fibrous materials $1 < \rho_a/\rho_0 < 4.5$. Usually k_s is close to unity for fine fibered, highly porous materials, the finer the fiber the lower the value for a given porosity. Actually k_s and Ω must be interrelated but the exact functional form is not important here.

Both internal inertial and frictional coupling can take place between the air motion and frame motion as mentioned above. Only internal coupling will be

considered even though some wave coupling can take place at both surfaces if the material is of finite depth ⁽²⁾. Boundary value problems will not be formulated until specific applications are considered.

For harmonic compressional waves of the form $\exp[-i(\Gamma x - \omega t)]$ the important inertial frictional coupling parameter in the theory of Zwicker and Kosten⁽²⁾ is here designated as

$$S_{12} = \omega \left[\frac{\rho_0(k_s - 1)}{\Omega} \right] + i\Phi = \omega \rho_{ei} + i\Phi \quad (3)$$

where ρ_{ei} is a density and Φ is a specific flow resistance (rayls per unit length). For most fibrous blanket materials $k_s \leq 4$. At low frequencies where $\omega \rho_{ei} \ll \Phi$ the internal coupling is primarily frictional.

Also define an effective density of the structural frame ρ_{es} as

$$\rho_{es} \equiv \rho_s \frac{(1 - \Omega)}{\Omega^2} + \rho_0 \frac{(k_s - 1)}{\Omega} \quad (4)$$

where ρ_s is the density of the bulk fibers. This definition incorporates ρ_{ei} where $\rho_{ei} < \rho_s (1 - \Omega)/\Omega^2$ even for porous materials for which $\Omega > 0.95$ and $k_s \leq 4$.

The ratio ρ_{es}/ρ_a is an important parameter in the theory of internal wave coupling. It is an index of the potential for appreciable acoustical energy storage in the frame as compared to the air in the pores of the frame.

The flow resistance Φ , Eq. 3, is not independent of either k_s or Ω . If the fibers are layered, a one-dimensional wave model with propagation normal to the direction of the fibers suffices, provided Φ is specified in the same direction. Likewise for propagation along the fibers. No attempt will be made here to introduce anisotropy and derive a three-dimensional wave

equation. Propagation normal to the fiber corresponds closely to some applications.

The propagation constant Γ corresponding to one-dimensional wave motion, will be complex number $\beta + i\alpha$ whose individual properties are important.

The dynamical equations of motion including the force equation and equations of continuity have been reformulated to reflect these definitions and also to identify important coupling parameters. (See Appendix B)

For the elastic frame the force equation can be expressed as

$$\frac{1 - \Omega}{\Omega} \Gamma P_S = \Omega [\omega_{p_{es}} + i\Phi] V_S - [\omega_{p_{ei}} + i\Phi] V_a . \quad (5a)$$

By using definitions put forth by Kosten and Janssen⁽¹⁰⁾ the equation of continuity becomes

$$\omega \kappa_S (1 - \Omega) P_S = \kappa_{11} \Gamma V_S + \kappa_{12} \Gamma V_a \quad (5b)$$

where

$$\kappa_{11} \equiv 1 + \left(\frac{1 - \Omega}{\Omega} \right)^2 \left(\frac{\Omega \kappa_S}{\kappa_a} \right) (1 - P_0 \kappa_a)$$

and

$$\kappa_{12} \equiv \frac{(1 - \Omega)}{\Omega^2} \left(\frac{\Omega \kappa_S}{\kappa_a} \right) .$$

The variables P_S and P_a are the complex acoustic pressure amplitudes in the frame structure and in the air, respectively, while V_S and V_a are complex particle velocity amplitudes. These variables are taken as averaged values over areas large compared to a "mean pore size". The precise way that average is computed is not clear.

where in addition the parameters

$$S_{11} \equiv \Omega (\omega \rho_{es} + i\Phi)$$

$$S_{22} \equiv \omega \rho_a + i\Phi$$

$$\sigma_{11} \equiv \omega \kappa_s (1 - \Omega)$$

$$\sigma_{22} \equiv \omega \kappa_a \Omega$$

and

$$S_{21} \equiv \Omega (\omega \rho_{ei} + i\Phi) = \Omega S_{12}.$$

First note that both Eqs. 5 and 6 reduce to their proper forms as either $\Omega \rightarrow 0$ or $\Omega \rightarrow 1$. Second, the matrix of wave coefficient in Eq. 7 has a certain symmetry with the inertial-frictional terms in the upper right hand corner, the elastic terms in the lower left hand corner, and the dilatational terms in the lower right hand corner. Notably, absent in this formulation are any terms corresponding to elastic cross coupling, i.e., $\sigma_{12} = \sigma_{21} = 0$.

Observe, however, that the κ 's do contain elastic constants and the relative importance of say κ_{12} depends on both Ω and the elastic ratio κ_s/κ_a . It also turns out that $\kappa_{11} \approx 1$ for highly porous, bulk materials and both κ_{12} and κ_{21} can be quite small compared to unity, in fact $\kappa_{12} \equiv 0$ if $\kappa_a = 1/P_0$. So all in all no significant elastic wave coupling is present in the theory of Zwikker and Kosten. Note further that since $\kappa_{11} \kappa_{22} - \kappa_{12} \kappa_{21} = 1$ any dilatational coupling that exists is

reciprocal.

There will exist four values for the propagation constant Γ corresponding to the coupled motion and waves travelling in both positive and negative x directions. Many aspects of the solution for Γ have been discussed by Zwicker and Kosten⁽²⁾ and somewhat later by Beranek⁽⁴⁾ and McGrath⁽¹¹⁾ and their interpretations will not be repeated here. By setting the determinant of the matrix of Eq. 7 equal to 0 one obtains for the characteristic equation

$$\begin{aligned} \Gamma^4 - \left[\kappa_{11} \sigma_{22} S_{22} + \frac{\Omega}{1 - \Omega} \kappa_{22} \sigma_{11} S_{11} + \kappa_{12} S_{21} \sigma_{22} \right. \\ \left. + \frac{\Omega}{1 - \Omega} \kappa_{21} S_{12} \sigma_{11} \right] \Gamma^2 + \frac{\Omega}{1 - \Omega} \kappa_{22} \sigma_{11} \sigma_{22} (S_{11} S_{22} - S_{12} S_{21}) = 0 \end{aligned} \quad (8)$$

since $\kappa_{11} \kappa_{22} - \kappa_{12} \kappa_{21} = 1$.

It is very tempting to drop cross-coupling terms like $\kappa_{12} S_{21} \sigma_{22}$, $\kappa_{21} S_{12} \sigma_{11}$, and $S_{12} S_{21}$ in comparison with other terms, in which case Eq. 8 factors and the waves types are completely decoupled. However, not all of these terms are negligible in any given situation. It is still instructive to establish a few criteria that facilitate approximate solutions of Eq. 8 and identify the propagation constant for sound waves in the air Γ_a and sound waves in the structure Γ_s when possible. For that purpose, one need only consider wave propagation in the positive x - direction.

First, note that the inequality

$$\kappa_{12} S_{21} \sigma_{22} + \frac{\Omega}{1 - \Omega} \kappa_{21} S_{12} \sigma_{11} < \kappa_{11} S_{22} \sigma_{22} + \frac{\Omega}{1 - \Omega} \kappa_{22} S_{11} \sigma_{11} \quad (9)$$

is valid provided

$$\left(\frac{1 - \Omega}{\Omega} \right)^2 (2 - P_0 \kappa_a) (Q_{ei}^2 + 1) < \left[\kappa_{11} \frac{\kappa_a}{\Omega \kappa_s} Q_a + Q_{es} \right]^2 + \left[1 + \kappa_{11} \left(\frac{\kappa_a}{\Omega \kappa_s} \right) \right]^2 \quad (10)$$

where $Q_{ei} \equiv \omega \rho_{ei} / \Phi$, $Q_a \equiv \omega \rho_a / \Phi$, and $Q_{es} \equiv \omega \rho_{es} / \Phi$ are convenient parameters for analysis.

This inequality is valid for all highly porous materials regardless of the value of the elastic ratio $\Omega \kappa_s / \kappa_a$ and at all frequencies of interest in the audio range. Moreover, since $\rho_{es} \gg \rho_a$ for $k_s \leq 4$ and reasonable values for ρ_s , frequency is no limitation. In the experiments to be described later the value of the left hand side of the inequality is about 0.007 for $P_o \kappa_a = \frac{1}{Y}$ and $\Omega = 0.94$. The lowest value for Q_{es} was 2.5. Unfortunately, there is no precise information about $\Omega \kappa_s / \kappa_a$ for the materials studied but the best judgement is that $\Omega \kappa_s / \kappa_a \gg 1$ over most of the frequency range of interest. The conclusion is that all of the cross-coupling terms in the coefficient for r^2 in Eq. 8 can be neglected.

The other requirement to be satisfied in order to eliminate cross-coupling entirely is that

$$S_{12} S_{21} < S_{11} S_{22} \quad (11)$$

in Eq. 8. This inequality reduces for $Q_{ei}^2 \ll 1$ to

$$1 < (Q_{es}^2 + 1) (Q_a^2 + 1) \quad (12)$$

which is more difficult to meet than Eq. 10 by orders of magnitude at low frequencies, say below 300 Hz. The requirement is met in the experimental situation at frequencies above say 1200 Hz. The conclusion is that the coupling terms $S_{12} S_{21}$ in Eq. 8 cannot safely be neglected at all frequencies of interest.

In order to obtain a solution to Eq. 8 valid over the entire range of frequencies of interest consider the requirement that

$$4 \frac{\Omega}{1-\Omega} \kappa_{22} \sigma_{11} \sigma_{22} (S_{11} S_{22} - S_{12} S_{21}) < \left[\kappa_{11} S_{22} \sigma_{22} + \frac{\Omega}{1-\Omega} \kappa_{22} S_{11} \sigma_{11} \right]^2 \quad (13)$$

Again, under the assumptions that $Q_{ei}^2 \ll 1$ and $\kappa_{11} \approx 1$ this inequality is valid provided both

$$\frac{\rho_a}{\rho_{es}} + \left(\frac{\Omega \kappa_s}{\kappa_a} \right)^2 > \left(\frac{\Omega \kappa_s}{\kappa_a} \right) \left(1 + \frac{\rho_a}{\rho_{es}} \right) \quad (14a)$$

and

$$\left(\frac{\rho_a}{\rho_{es}} \right)^2 + \left(\frac{\Omega \kappa_s}{\kappa_a} \right)^2 > 2 \frac{\rho_a}{\rho_{es}} \left(\frac{\Omega \kappa_s}{\kappa_a} \right) \quad (14b)$$

which can be met under certain conditions. There are two extreme conditions in the relative values of the ratios $\Omega \kappa_s / \kappa_a$ and ρ_{es} / ρ_a that will satisfy both requirements. The first is the so-called "flexible blanket" frame condition where

$$\frac{\Omega \kappa_s}{\kappa_a} \gg 2 \rho_a / \rho_{es} \quad (15)$$

or $c_a^2 / c_s^2 \gg 2$ where $c_a^2 \equiv (\rho_a \kappa_a \Omega)^{-1}$

and $c_s^2 (\rho_{es} \kappa_s \Omega^2)^{-1}$. Here c_a is identified as the speed of sound in the air of the pores and c_s is the speed of compressional elastic waves in the frame. Eq. 15 is easily satisfied for most highly porous flexible blanket materials over wide ranges of frequency.

The second extreme condition is the so-called "stiff frame" condition where

$$\frac{\kappa_a}{\Omega \kappa_s} \gg \rho_{es}/2\rho_a \quad (16)$$

or $c_a^2/c_s^2 < 2$ which probably is a more difficult condition to satisfy over a wide range of frequencies. From equations 2 and 4,

$\frac{\rho_{es}}{\rho_a} = \frac{\rho_s}{\rho_0} \frac{(1 - \Omega)}{\Omega \kappa_s} + \frac{\kappa_s - 1}{\kappa_s}$, which for many porous materials including flexible blankets is a number much greater than unity. For one type of Kevlar 29, the ratio $\rho_{es}/\rho_a \approx 40$ based on a value of $\kappa_s = 2.1$ while for Scottfoam $\rho_{es}/\rho_a \approx 13$ based on a value of $\kappa_s = 2.1$ and numerical values of ρ_s for each material (see Table I). It appears on the basis of measurements by others, notably Beranek⁽⁴⁾, that commercial materials which are acoustically stiff at low frequencies lose that quality at high frequencies, i.e. the ratio $\Omega \kappa_s/\kappa_a$ is highly frequency dependent for some materials notably stiff acoustical tiles or boards.

Solutions of Eq. 8 are quite different depending rather critically on choices for the stiffness ratio $\Omega \kappa_s/\kappa_a$ and the density ratio ρ_{es}/ρ_a . Again note that κ_{11} contains $\Omega \kappa_s/\kappa_a$ as a parameter but unless $\Omega \kappa_s/\kappa_a$ is extremely large say greater than 50 and κ_a is adiabatic the value of κ_{11} will remain close to unity. If κ_a remains isothermal at all frequencies its value is unity.

It is not worthwhile speculating further about the relative values of κ_s and κ_a until more information about κ_s for spun fiber and open-cell foam materials is available. It is doubtful that static values of κ_s will suffice and at best would provide a bound on $\Omega \kappa_s/\kappa_a$. No concerted effort to find dynamic values of κ_s for highly porous, acoustical materials has been made.

to-date. Also, such information is not provided by the manufacturers of acoustical materials on a routine basis. Instead, it will be assumed that the conditions of Eq. 13 obtain and then proceed to find approximate solutions for Γ .

B. Propagation Parameters

If the conditions of Eq. 13 are satisfied then the two solutions to Eq. 8 can be expressed as

$$\Gamma_-^2 \approx \kappa_{22} \frac{\Omega}{1-\Omega} \sigma_{11} \sigma_{22} \frac{(S_{11} S_{22} - S_{12} S_{21})}{\kappa_{11} \sigma_{22} S_{22} + \frac{\Omega}{1-\Omega} \kappa_{22} \sigma_{11} S_{11}} \quad (17a)$$

and

$$\Gamma_+^2 \approx \kappa_{11} \sigma_{22} S_{22} + \kappa_{22} \frac{\Omega}{1-\Omega} \sigma_{11} S_{11} - \Gamma_-^2 \quad (17b)$$

At this point one cannot identify whether Γ_- is associated primarily with wave motion in the elastic frame or sound waves in the air pores and likewise for Γ_+ . However, if the conditions of either Eqs. 15 or 16 are imposed then the identification is readily made by comparison with exact solutions for decoupled motion.

It is convenient to rewrite Eq. 17a in the form

$$\Gamma_-^2 \approx \frac{\omega^2}{\kappa_{11} c_s^2} \left[\frac{\left(1 + \frac{i}{Q_{es}}\right) \left(1 + \frac{i}{Q_a}\right) - \frac{Q_{ei}^2}{Q_a Q_{es}} \left(1 + \frac{i}{Q_{ei}}\right)^2}{\left(1 + \frac{i}{Q_a}\right) + \frac{c_a^2}{\kappa_{11} c_s^2} \left(1 + \frac{i}{Q_{es}}\right)} \right] \quad (18)$$

Also, Eq. 17b becomes

$$\Gamma_+^2 \approx \frac{\omega^2}{c_a^2} \left(1 + \frac{i}{Q_a}\right) + \frac{\omega^2}{c_s^2} \left(1 + \frac{i}{Q_{es}}\right) - \Gamma_-^2$$

If conditions of Eq. 15 are satisfied then $c_a^2 \gg c_s^2$ and

$$\Gamma_-^2 = \Gamma_a^2 \approx \frac{\omega^2}{c_a^2} \left[\left(1 + \frac{i}{Q_a} \right) + \frac{1}{Q_a Q_{es}} \frac{1}{\left(1 + \frac{i}{Q_{es}} \right)} \right] \quad (20)$$

on the assumption that $Q_{ei}^2 \ll 1$. Likewise,

$$\begin{aligned} \Gamma_+^2 = \Gamma_s^2 \approx & \frac{\omega^2}{c_s^2} \left(1 + \frac{i}{Q_{es}} \right) - \frac{\omega^2}{c_a^2} \frac{1}{Q_a Q_{es}} \frac{1}{\left(1 + \frac{i}{Q_{es}} \right)} \\ & + (\kappa_{11} - 1) \frac{\omega^2}{c_a^2} \left(1 + \frac{i}{Q_a} \right) . \end{aligned} \quad (21)$$

Note, in the completely decoupled case that the sound waves in the pore space have a propagation constant

$$\Gamma_a^2 = \frac{\omega^2}{c_a^2} \left(1 + \frac{i}{Q_a} \right) \quad (22)$$

and the elastic waves in the structure have

$$\Gamma_s^2 = \frac{\omega^2}{c_s^2} \left(1 + \frac{i}{Q_{es}} \right) . \quad (23)$$

Thus, for the flexible blanket where $c_a^2 \gg c_s^2$, Γ_a is identified with Γ_- and Γ_s is identified with Γ_+ .

The most important effects of wave coupling are identified by examining equations 20 and 21 and noting that the effective wave speeds and internal damping are modified by terms that involve the product $Q_{es} Q_a$. (See Appendix A for a more precise analysis.) Since $c_a^2 \gg c_s^2$ and $\kappa_{11} \approx 1$, the last two terms in Eq. 21 usually are dropped and the expression for Γ_s simplifies

to the decoupled case. Also, Eq. 20, can be expressed in terms of Q_{es} and ρ_{es}/ρ_a as

$$\Gamma_a^2 \approx \frac{\omega^2}{c_a^2} \left[1 + \left(\frac{\rho_{es}}{\rho_a} \right) \frac{1}{Q_{es}^2 + 1} + i \left(\frac{\rho_{es}}{\rho_a} \right) \frac{Q_{es}}{Q_{es}^2 + 1} \right] \quad (24)$$

which is a convenient form for parametric analysis and numerical computations if coupled motion is important.

All of the parameters in Eq. 24 are presumed known or can be obtained from independent measurements. Values of ϕ for Kevlar 29 and Scottfoam are available^(6,7,8). However, values of k_s are more difficult to establish and c_a , ρ_{es}/ρ_a and Q_{es} are dependent on that value. It is a very important parameter to establish in the theory of Zwikker and Kosten. No assumption about the value of κ_a has been made except that it has been treated as a real number. It is pure real at either very low or very high frequencies but at intermediate values it is a complex number. In the parametric analysis it will be presumed known at high frequencies, either adiabatic or isothermal. It is expected that if there is appreciable mechanical damping in the fibers of the frame that κ_s also will be a complex number. Fortunately, in the parameteric analysis a precise value did not have to be established.

The "stiff frame" conditions of equation 16 is interesting and useful for better understanding of porous acoustical materials. If $\kappa_a/\Omega\kappa_s \gg 2 \rho_{es}/\rho_a$, say greater than 50, then $c_s^2 \gg c_a^2$ and this theory predicts that

$$\Gamma_-^2 = \Gamma_s^2 \approx \frac{\omega^2}{\kappa_{11} c_s^2} \left[\left(1 + \frac{i}{Q_{es}} \right) - \frac{Q_{ei}^2}{Q_a Q_{es}} \left(\frac{1 + \frac{i}{Q_{ei}}}{1 + \frac{i}{Q_a}} \right)^2 \right] \quad (25)$$

and

$$\Gamma_+^2 = \Gamma_a^2 \approx \frac{\kappa_{11}\omega^2}{c_a^2} \left(1 + \frac{i}{Q_a}\right) - \frac{\omega^2}{c_s^2} \left[\frac{i}{\kappa_{11} Q_{es} Q_a \left(1 + \frac{i}{Q_a}\right)} - (1 - \kappa_{11}) \left(1 + \frac{i}{Q_{es}}\right) \right] \quad (26)$$

where now $\kappa_{11} \neq 1$ unless $\kappa_a = 1/P_0$. Again, the expression

for Γ_a can be simplified by dropping the last two terms which is fairly good approximation if $\frac{\kappa_a}{\Omega\kappa_s} \gg 2\rho_{es}/\rho_a$. Then Γ_a^2 reduces to that for decoupled motion with slight modifications in that $\kappa_{11} \neq 1$.

Note, also that the roles of Γ_- and Γ_+ have interchanged from that of the "flexible" porous blanket. In effect, there is a switching regime due to internal wave coupling which is most likely a frequency dependent phenomenon. Just how and where this switching occurs depends on the detailed behavior of $\Omega\kappa_s/\kappa_a$.

On the basis of experimental information now available it appears that the inequality $\frac{\kappa_a}{\Omega\kappa_s} \gg \rho_{es}/2\rho_a$ obtains for rigid board type materials at low frequencies i.e. $Q_{es}^2 \ll 1$. At high frequencies it does not seem to matter whether the porous material is rigid or not and the waves decouple in any event. Predictions are then fairly readily made and there is good agreement among various workers. Delany and Bagley⁽¹²⁾ have noted this and characterized a wide range of fibrous absorbent materials on the basis of a single parameter such as ω/Φ . They used various grades of glass fibers and mineral wool materials and found an excellent empirical fit over a range of frequencies from 250 to 4000 Hz which includes the range used in this study. However, at sufficiently low frequencies there is appreciable wave interaction and it is doubtful that such a simple characterization is possible. This is undoubtedly the case where the structure factor k_s is greater than 4.

Zwikker and Kosten⁽²⁾ have discussed some of these matters in detail and conclude that the frequency above which coupling forces are likely to be insignificant is given by

$$\omega^1 \left[\rho_s \left(\frac{1 - \Omega}{\Omega^2} \right) + \frac{\rho_o (k_s - 1)}{\Omega} \right] = \phi \quad (27)$$

where ω^1 is designated as a decoupling frequency. For Kevlar 29 using $k_s \approx 3$ this frequency is about 130 Hz which is well below the lowest frequency used, namely 300 Hz. For Scottfoam it is about 85 Hz for $k_s \approx 2$.

It should be noted that for conditions where $Q_{es}^2 \gg 1$, both the "stiff frame" and the "flexible blanket" approximations yield identical results, i.e., Eq. 26 becomes identical with Eq. 20. However, at lower frequencies, say $Q_{es} < 3$ there is considerable discrepancy, see Figures 1 and 2. Experimental facilities were not available to check the low range of frequencies (below 300 Hz) directly for either Kevlar or Scottfoam.

Shown in Figure 1 is a plot of the normalized propagation constant $c_a/\omega\Gamma_a = B + iA$ as a function of Q_{es} based on Eq. 24 for $\rho_{es}/\rho_a = 38$. Also shown for comparison purposes are results predicted by Eq. 22 based on completely decoupled motion. Note,* the large discrepancies for the range $Q_{es} < 4$ especially in the attenuation component. On this basis any analysis based on decoupled wave motion will overpredict the attenuation and underpredict the phase shift primarily at low frequencies. It also should be noted that the greater the ratio ρ_{es}/ρ_a the more sensitive the motion is to internal wave coupling. Further, it should be noted that the real and imaginary part of Γ_a at a given frequency are not in general equal unless the waves are decoupled and Q_{es} is low, say less than 4. In particular, A and B are not equal for large Q_{es} . This judgement is based on the

assumption that $\rho_{es}/\rho_a > 10$.

In closing this discussion it is interesting and useful to point out that the general results are compatible with earlier work by Beranek⁽⁴⁾ except that he employed some different definitions. He studied the properties of both "flexible blanket" and "rigid tile" and expressed his results in terms of an "effective density" ρ_e which is different from ρ_a and a dynamic resistance here called ϕ_e . This matter is discussed in the appendix. The two analyses are brought into better quantitative agreement if $\rho_e \Omega$ becomes $\langle \rho_1 \rangle$ in Beranek's work. The qualitative results are for all intents and purposes the same.

In the following section the acoustical impedance and sound absorption coefficient relationships for bulk materials will be discussed briefly.

III. Impedance and Absorption Relationships

The utilization of the coupled equations of motion to predict acoustical impedance of absorptive materials has been discussed by Zwicker and Kosten⁽²⁾, Kosten and Janssen⁽¹⁰⁾ and Beranek⁽⁴⁾ in great detail. Generally speaking the analyses are very complex and difficult to follow in detail. Here, an approximate method is employed which yields good results in the "weak coupling" cases. In such cases the coupling terms in the dynamical equations of motion are dropped completely and the impedance for the sound waves in the air of the pores becomes

$$Z_a \approx \frac{\omega \rho_a + i\phi}{\Gamma_a} \quad (28)$$

on the basis of Eq. 6a and for waves in the elastic frame

$$Z_s \approx \frac{\Omega^2}{(1 - \Omega)} \frac{\omega \rho_{es} + i\phi}{\Gamma_s} \quad (29)$$

on the basis of Eq. 5a.

Any effects of wave coupling then enter only through the modified values of Γ_a and Γ_s .

According to Kosten and Janssen⁽¹⁰⁾ this can be done quite rigorously when the frame is either very flexible or very stiff by very careful approximations. But, apparently this procedure cannot be followed in intermediate situations where $c_a^2 \approx c_s^2$. Thus, if the condition imposed is either $c_a^2 \gg c_s^2$ or $c_a^2 \ll c_s^2$ then Eqs. 28 and 29 can be employed to determine the impedances.

Here it will be assumed that the "flexible blanket" condition obtains, Eq. 15, and one predicts that

$$Z_a \approx \rho_a c_a \frac{(1 + i/Q_a)}{\left[1 + \left(\frac{\rho_{es}}{\rho_a} \right) \frac{1}{(Q_{es}^2 + 1)} + i \left(\frac{\rho_{es}}{\rho_a} \right) \frac{Q_{es}}{Q_{es}^2 + 1} \right]^{1/2}} \quad (30)$$

and

$$Z_s \approx \rho_s c_s \frac{(1 + i/Q_{es})}{\left[\left(1 + \frac{i}{Q_{es}} \right) - \left(\frac{c_s^2}{c_a^2} \right) \frac{1}{Q_a Q_{es}} \frac{1}{(1 + i/Q_{es})} + (\kappa_{11} - 1) \left(\frac{c_s^2}{c_a^2} \right) \left(1 + \frac{i}{Q_a} \right) \right]^{1/2}} \quad (31)$$

The form of Eq. 31 is not particularly useful since we do not have information about the ratio c_s^2/c_a^2 . So usually c_s^2/c_a^2 is taken small compared with unity for flexible blankets and then for reasonable values of Q_{es} and Q_a the last two terms in the denominator of Eq. 31 are dropped.

The total surface admittance of a sample of bulk porous material is

$$Y \approx Y_s + Y_a \quad \text{where the area weighting has been taken into account.}$$

Since $\rho_s c_s \gg \rho_a c_a$ one can establish that $|Y_s| \ll |Y_a|$ and the admittance of the sample is that due to the air motion alone.

Obviously there are restrictions on both ρ_{es}/ρ_a and

ρ_{es}/ρ_a for this to be the case. The approximation presents a great simplification and it usually is made in most applications of porous materials and in other applications like predicting the influence of ground on the absorption and reflection of sound.

Then the normalized impedance of the surface of a bulk material becomes

$$\frac{Z_a}{\rho_0 c_0} = \frac{\sqrt{k}}{\Omega} \frac{\left(1 + i \frac{\rho_{es}}{\rho_a} \frac{1}{Q_{es}}\right)}{\left[1 + \left(\frac{\rho_{es}}{\rho_a}\right) \frac{1}{Q_{es}^2 + 1} + i \left(\frac{\rho_{es}}{\rho_a}\right) \frac{Q_{es}}{Q_{es}^2 + 1}\right]^{1/2}} \quad (32)$$

where c_0 is the adiabatic speed of sound and the parameter $k = k_s / \kappa_a P_0 \gamma$.

First, one notes that in general quite a large number of parameters are required to characterize the impedance properties of the porous material.

At least four stand out explicitly, namely k , Ω , ρ_{es}/ρ_a , and Q_{es} .

Recall that $\rho_{es}/\rho_a = \frac{\rho_s (1 - \Omega)}{\rho_0 k_s} + \frac{k_s - 1}{k_s}$. Also $Q_{es} = \omega \rho_{es}/\phi$ requiring knowledge of the specific flow resistance ϕ . This is a larger number of parameters than usually employed.

The structural factor k_s enters into all of the parameters namely k , ρ_{es}/ρ_a and Q_{es} . However, if wave coupling is neglected then Eq. 32 simplifies and can be expressed as

$$\frac{Z_a}{\rho_0 c_0} = \frac{R_a}{\rho_0 c_0} - i \frac{X_a}{\rho_0 c_0} \approx \frac{\sqrt{k}}{\Omega} \left(1 + i \frac{1}{Q_a}\right)^{1/2} \quad (33)$$

where $Q_a = \omega \rho_a / \phi = \omega \rho_0 (k_s / \Omega \phi)$.

Now k_s enters into only two parameters, k and Q_a . The high frequency asymptote in both Eqs. 32 and 33 is \sqrt{k}/Ω . If κ_a is known at high frequencies then k_s can be established uniquely, in principle.

The normal incidence sound absorption coefficient α_a can be expressed in terms of the surface impedance and becomes for highly porous bulk samples namely

$$\alpha_a = \frac{4 (R_a / \rho_0 c_0)}{(1 + R_a / \rho_0 c_0)^2 + (X_a / \rho_0 c_0)^2} \quad (34)$$

Generally speaking α_a requires as many parameters as Z_a in order to describe its behavior.

If normal impedance measurements are made on samples of porous material of finite depth ℓ backed by a plate that presents an acoustic impedance large compared to $\rho_a c_a$ then the impedance of the surface is modified to read

$$\frac{Z_{in}}{\rho_0 c_0} = \frac{R_{in}}{\rho_0 c_0} - i \frac{X_{in}}{\rho_0 c_0} = \frac{Z_a}{\rho_0 c_0} \coth(-i\Gamma_a \ell) \quad (35)$$

where $\Gamma_a = \beta_a + i \alpha_a$ For computational purposes Eq. 35 can be expressed as

$$\frac{R_{in}}{\rho_0 c_0} = \frac{(R_a/\rho_0 c_0) \sinh(\alpha_a \ell) \cosh(\alpha_a \ell) + (X_a/\rho_0 c_0) \sin(\beta_a \ell) \cos(\beta_a \ell)}{\cosh^2(\alpha_a \ell) - \cos^2(\beta_a \ell)} \quad (36a)$$

and

$$\frac{X_{in}}{\rho_0 c_0} = \frac{(X_a/\rho_0 c_0) \sinh(\alpha_a \ell) \cosh(\alpha_a \ell) - (R_a/\rho_0 c_0) \sin(\beta_a \ell) \cos(\beta_a \ell)}{\cosh^2(\alpha_a \ell) - \cos^2(\beta_a \ell)} \quad (36b)$$

If, at a given frequency $\alpha_a \ell$ is taken so large that $\tanh(\alpha_a \ell) \geq 0.998$, which obtains for $\alpha_a \ell \geq 3.6$, then for all practical purposes $R_a = R_{in}$ and $X_a = X_{in}$. This condition was met or exceeded for the range of frequencies used in this study.

A representative plot of $R_a/\rho_0 c_0$ and $X_a/\rho_0 c_0$ for Kevlar 29 is shown in Figures 2a and 2b, respectively. Again note, the range of Q_{es} for which the decoupled wave approximation is valid.

In the following section a method for establishing the value for the structure constant k_s is presented. Also, a brief summary of some previous work endeavoring to relate Φ , k_s and Ω will be given.

IV. Parametric Studies

While there are a number of ways of describing the impedance and absorptive properties of bulk porous material one would prefer to employ as few parameters as possible. In particular it is advantageous to characterize both the real and imaginary part of the impedance so as to be able to predict just what physical properties essentially control their behavior. One then could select optimum values for all parameters in order to achieve a desired impedance or absorptive characteristic, if possible. Also there are hidden parameters such as temperature to which the impedance and absorption could be sensitive.

Some attempts have been made to characterize the impedance properties of fibrous absorbent materials by a single parametric ratio such as ω/Φ . This may be possible if the structural characteristics of the candidate materials all have about the same \sqrt{k}/Ω values.

The impedance of a bulk sample of a porous flexible material is given in Eqs. 32 and 33 where the high frequency resistance is

$$\frac{\sqrt{k}}{\Omega} = \sqrt{\frac{\rho_a}{\rho_0} \left(\frac{1}{\kappa_a P_0 \gamma} \right) \frac{1}{\Omega}} \quad (38)$$

In the theory of Zwikker and Kosten $\rho_a/\rho_0 = k_s/\Omega$ and κ_a is assumed known at high frequencies.

Some workers prefer to let $\rho_a/\rho_0 = m$ where m also is interpreted as a structure factor.

Then

$$\frac{\sqrt{k}}{\Omega} = \sqrt{\frac{k_a}{\Omega}} \quad (39)$$

where $k_a = m$ if $\kappa_a = \frac{1}{\rho_0 \gamma}$ and $k_a = \frac{m}{\gamma}$ if $\kappa_a = \frac{1}{p_0}$. In most characterizations m is interpreted as a function of the porosity alone.

Note also that the speed of sound in the air of the pores

$$c_a^2 = \frac{1}{\kappa_a \rho_a \Omega} = c_0^2 / k_s$$

where $c_0^2 = \frac{1}{\kappa_a \rho_0}$ is the speed of sound in the air of the pores if the air motion is unrestricted. However, there appears to be no immediate advantage in characterizing behavior of the material by simply redefining ρ_a / ρ_0 so the definition in Eq. 2 is retained.

It is surmised that the parameters Φ , Ω and k_s are interrelated but the question as to how probably cannot be settled as a purely empirical basis. In the theory of Zwikker and Kosten, the specific flow resistance Φ is independent of frequency in the audio range. A precise definition of low and high frequency behavior is not available for most materials but it appears for highly porous, fibrous materials including open cell foams that the acoustic Reynolds number $\omega d^2 / \nu$ must be less than unity in order for Φ to be independent of frequency. Here d is a mean diameter of the fibrous filament and ν is the coefficient of kinematic viscosity for air surrounding the fibers. The average spacing between fibers must be sufficiently great so that there is no interaction between fibers. If the open-cell foam consists of solid filaments of mean diameter d with a mean separation $D \gg d$, then it is likely to have a comparable index⁽¹³⁾.

On the basis of experimental data available it appears that Φ for Kevlar 29 and Scottfoam is constant in the frequency range below 3000 Hz. However, at high frequencies, where $\omega d^2 / \nu > 1$, it appears on a theoretical basis employing simple acoustic boundary layer theory that Φ should vary as $\sqrt{\omega}$. R. W. Morse⁽⁵⁾ has predicted for acoustic wave propagation in porous media

modelled as ensembles of small tubes that

$$\frac{\Omega\Phi}{k_s} \propto \nu\rho_0/d^2, \quad \omega d^2/\nu < < 1 \quad (40a)$$

and

$$\frac{\Omega\Phi}{k_s} \propto \sqrt{\frac{2\mu\rho_0\omega}{d}}, \quad \omega d^2/\nu > > 1 \quad (40b)$$

where d is the diameter of the tubes and $\mu = \rho_0 \nu$

The constant of proportionality in Eq. 40 is important and likely to vary from one material to another. More recently Hersh and Walker⁽⁷⁾ have shown in the basis of a one-dimensional layered fiber model for Kevlar 29 that

$$\frac{\Omega\Phi}{k_s} = (\nu\rho_0/d^2) \frac{\left[1 + K \sqrt{\frac{\Pi}{4(1-\Omega)}}\right]}{K \left[\frac{\Pi}{4(1-\Omega)}\right]^{3/2}} \quad (41)$$

where $K = .059$ is an empirical constant. In their work it does not appear possible to isolate Φ , Ω , and k_s . This representation then agrees fairly well with their data over the frequency range 100 to 2000 Hz. It is interesting to note that the theory of Zwikker and Kosten can be brought into substantial agreement with the work of others by such an identification but generally there is an empirical constant to fit. In the parametric work of this paper values for Φ and Ω were considered known and a single parameter k_s selected to provide a fit of the data over the entire frequency range.

In order to establish a value for k_s parametric plots of Eq. 33 based on decoupled motion were made employing Q_a as a variable and $\sqrt{k/\Omega}$ as a parameter. Initially κ_a was selected to be adiabatic and $\sqrt{k/\Omega}$ determined from the high frequency asymptote. That provided an initial estimate of k_s . Then Q_a values were calculated and the data plotted against the parametric plots. A new value for $\sqrt{k/\Omega}$ was then established on the basis of comparisons of the $R_a/\rho_0 c_0$, $X_a/\rho_0 c_0$ and α_a data with the predictions. This provided a correction to the k_s value. It was not possible to choose a single value for k_s that fit both the high frequency and low frequency data for all types of materials. One reason may be that κ_a varies from its isothermal to adiabatic value as frequency increases. The most satisfactory fit to the low Φ Kevlar and Scottfoam data, especially the reactive component of impedance, was obtained by selecting κ_a to be isothermal at all frequencies and then slightly adjusting k_s to fit the low frequency data. This procedure also is the most satisfactory for fitting sound absorption data, Fig. 12. The fit to the resistive component at all frequencies is then not so good as desired. Another reason may be wave coupling at the lower frequencies that invalidates the parametric procedure. There are some noticeable differences between Kevlar and Scottfoam in this respect. No attempt was made to alter the values of Φ and Ω in the procedure, only k_s .

The parametric curves based on Eq. 33 are shown in Figs. 3, 4, and 5. The range of parameters $0.9 \leq \sqrt{k/\Omega} \leq 2$ was preselected because most highly porous fibrous materials would fall in this range. Some fibrous materials having large values of k_s and low values of Ω may fall outside but are not likely candidates for most noise control applications. It may be possible to develop materials for which $\sqrt{k/\Omega} < 1$ which is highly desirable at

low frequencies, but they would require low values of k_s and high values of Ω . It is doubtful, in any event, that \sqrt{k}/Ω would ever be less than $1/\gamma^{1/2} = .845$ for air. Also if one were interested in predicting the absorptive properties of porous ground cover perhaps a different set of \sqrt{k}/Ω values would have to be considered.

Finally, parametric curves based on coupled wave motion could be plotted against Q_{es} in other applications especially these involving extremely low frequencies, say $Q_{es} < 2$ or 3 . Such parametric curves might be more useful for engineering design where specific values for either $R_a/\rho_0 c_0$ or $X_a/\rho_0 c_0$ (or both) are desired from a bulk absorbent material. No attempt has been made to fit the measured data to a parametric set of curves based on Eq. (32) as of this data. Parametric curves should be developed for coupled, Eq. (32), as well as decoupled, Eq. (33), wave motion. Results based on the parametric studies are presented in Table I.

In the following sections the experimental results will be presented together with a discussion based on comparisons with decoupled wave motion.

V. Experimental Results and Discussions

An experimental program was undertaken in order to determine the impedance and absorptive properties of two types of Kevlar 29 that were available. One type is a light weight blanket that appears to have a layered structure that can be easily separated. The other type is a more dense blanket that appears to have a woven structure and cannot be separated. The fibers appear to be the same in both types. The acoustical properties of the two types are quite different, the light weight blanket has a comparatively low value of flow resistance while the dense blanket has a higher value of ϕ , see Table I. Values of ϕ for Kevlar had been established earlier by Smith and Parrott⁽⁶⁾ and Hersh and Walker⁽⁷⁾.

Also available were samples of an open-cell foam material called Scottfoam. Its propagation and impedance properties had been studied and were available for comparison purposes⁽⁸⁾. No detailed comparisons and discussion of propagation contains for either Kevlar or Scottfoam will be presented in this report. It did turn out that the theory of Zwicker and Kosten overpredicts the attenuation and underpredicts the phase constant slightly in the frequency range 300 to 3000 Hz for high ϕ Kevlar 29 based on the parameter values presented in Table I. Experimental values of attenuation were used to determine the required depth of sample based on Eq. 36. The required depth of sample for Kevlar 29 was 12 cm while that used for Scottfoam was 25 cm.

No detailed description of the experimental apparatus and techniques employed will be presented here. All impedance and absorption measurements were made in a conventional impedance tube having an inside diameter of 5.72 cm. The samples were held securely in a special tube and faced with a highly porous screen at one end and a rigid impervious plug at the other. The technique employed plane waves to measure the standing wave ratio and positions

of the first minimum in the acoustic pressure standing wave patterns. The sound pressure level at the face of the sample was detected by a reference microphone and held constant. The standing wave detector was controlled by a dedicated digital computer which greatly facilitated the gathering of data and subsequent data reduction.

The measured values of normalized acoustical impedance and normal incidence absorption coefficient are shown in Figs. 6-12. The trends and levels are clearly established for the three specimens tested. The data were highly repeatable and followed typical patterns for porous, flexible blanket type materials. Some difficulties in holding the dense Kevlar discs were encountered but were overcome by compressing the samples slightly. This did have the effect of raising the high frequency asymptote $\sqrt{k/\Omega}$ from about 1.5 to 1.9 and corresponding reducing the absorption coefficients at all frequencies.

The parametric study established the values for the structure factor k_s shown in Table I. Other physical parameters used in the computations are included in the table for comparison purposes. The value of Φ for the light weight blanket Kevlar was computed from the data of Hersh and Walker, namely 46.4 cgs rayls. Their force equation neglects inertial wave coupling entirely by setting $k_s=1$. They then proceed to develop Eq. 41 where their structural parameter $K = 0.059$. If one then identifies $\Phi\Omega/k_s$ with their parameter σ the computed value is obtained. It is believed that the two formulations are self-consistent if this identification is made. When preparing samples of the low Φ Kevlar the porosity Ω was preselected as 0.94 to match the high Φ Kevlar and then the required amount of material was packed into the specimen holder to a depth of 12 cm.

The Scottfoam sample is an open-cell foam that under comparative examination with Kevlar has a fiber diameter about 1.667 times as great. If the published value of $d = 1.3 \times 10^{-3}$ cm for Kevlar 29 is correct then d for the Scottfoam is about 2.1×10^{-3} cm. This value for d then correlates very well with a measured value of $\phi = 18$ cgs rays.

The characteristics of $R_a/\rho_0 c_0$, $X_a/\rho_0 c_0$ and α_a were then computed using Eq. 33 and the values of the parameters in Table I. No further adjustments in any of the parameters were made and the results of these computations are plotted together with experimental data in Figs. 6-12. The predictions of $X_a/\rho_0 c_0$ agree very well with measured values for all samples. There are, however, some discrepancies in the predicted values of $R_a/\rho_0 c_0$ especially at low frequencies. The exact reason for this discrepancy which seems to be outside the range of experimental error is unknown as of this date. However, it was decided not to adjust k_s to provide a better fit to $R_a/\rho_0 c_0$ until a parametric study based on coupled wave motion is undertaken and completed.

Predicted values of absorption coefficient α_a are sensitive to small changes in $X_a/\rho_0 c_0$ and provide another index for comparison purposes. The agreement between theoretical values and experiment is excellent for both the low ϕ Kevlar and Scottfoam over a wide range of frequencies. The low ϕ Kevlar characteristics do depart in an intermediate frequency range providing some evidence that the samples were vibrating and absorbing energy.

Of special interest are the impedance and absorption characteristics of the high ϕ Kevlar, especially the larger value of k_s required to provide satisfactory agreement. This result was not entirely unexpected since the value of ϕ is higher also. Note, that ϕ and k_s are directly

proportional on the basis of theory of Morse, Eq. 40. Moreover, Morse⁽⁵⁾ predicted that the structure factor k_s will have a value of about 3 if the fibers are randomly oriented. He also reported values for k_s between 2 and 3.4 on the basis of measurements in granular porous media.

The other conclusion based on the parametric studies was that the thermodynamic process is essentially adiabatic at high frequencies for the high ϕ Kevlar. Selecting an isothermal value for κ_a , while providing a better fit to the $R_a/\rho_o c_o$ data, did not agree well with the $\chi_a/\rho_o c_o$ data being much too high, and correspondingly produced values of α_a that were much too low especially at high frequencies. It is concluded that the thermal process changed with frequency and a frequency dependent value for κ_a is required to provide a better fit of the data. It can be remarked with confidence that the two types of Kevlar behave quite differently both with regard to impedance and absorption. This matter would require more theoretical study based on very careful thermodynamic and structural considerations to provide a better rationale for the differences noted. Note, that both types had the same porosity.

On the other hand, the low ϕ Kevlar and Scottfoam samples do behave surprising alike in spite of quite different mechanical structure. The Scottfoam has a much lower ϕ , a lower material density ρ_s , and a lower structural to air density ratio ρ_{es}/ρ_a . However, the Q_a of Scottfoam is roughly twice that of Kevlar for the same value of k_s . This fact makes it a more efficient absorber at low frequencies even though \sqrt{k}/Ω is the same. In Fig. 12 the frequency range for Scottfoam is 500 to 3500 Hz while that for Kevlar is 300 to 3000 Hz.

When plotted versus Q_a the data of low ϕ Kevlar and Scottfoam

collapse to the same parametric curve. This is shown quite convincingly in the absorption characteristics, Fig. 12. The high Φ Kevlar data, on the other hand, follow a higher \sqrt{k}/Ω parameteric curve and display a correspondingly lower α_a characteristic. The ratio is just 1.9 to 1.3. All of the absorption data could be collapsed when normalized with respect to this ratio.

It is becoming common practice to plot absorption data versus a parameter such as Q_a (12, 14). The values of Q_a are then varied by changing frequency since Φ , k_s , and Ω are regarded as constants. The parameter Q_a can be interpreted as an energy ratio, namely of 2π times the maximum stored acoustic energy per unit volume of material to the energy dissipated per unit of time per unit of volume. Thus, it is very convenient parameter from an energy viewpoint. It also can be expressed as

$$Q_a = \frac{\omega \rho_a}{\Phi} = 2\pi \left(\frac{\rho_a c_a}{\lambda_a \Phi} \right) \quad (42)$$

where $\rho_a c_a$ is the acoustic impedance of the sample neglecting dissipation and λ_a is the acoustic wavelength within the material. Other interpretations may be possible. Therefore, it was decided to plot all data and make comparisons employing Q_a as a frequency variable.

VI. Summary and Recommendations

A. Results

(1) A theoretical formulation of acoustic wave propagation in porous elastic structures due to Zwikker and Kosten has been recast into a form that makes identification of various coupling parameters notably inertial, frictional, elastic, and dilatational more evident, see Eq. 7.

(2) Conditions under which the compressional elastic wave in the frame decouples from the acoustic wave in the air of the fibrous pores have been carefully examined. Weak coupling solutions have been formulated and expressed in terms of a frame structure quality factor Q_{es} which provides a convenient index, see Figs. 1 and 2.

(3) A density ratio ρ_{es}/ρ_a has been defined which plays an important role in the theory of wave coupling. The lower the values of this ratio the less susceptible the air acoustic wave is to the influence of energy storage in the elastic wave and vice versa. This ratio in conjunction with the stiffness ratio $\Omega\kappa_s/\kappa_a$ controls the nature of the wave coupling, see Eqs. 15 and 16.

(4) A new derivation of the expressions for equivalent density ρ_e and dynamic resistance for porous materials Φ_e has been developed. An equivalent quality factor Q_e also has been defined. This formulation could be used for a parametric analysis of materials where wave coupling is involved (see Appendix A.)

(5) Parametric curves for impedance and absorption coefficient based on decoupled wave motion have been prepared which facilitate identification of the structure factor k_s for flexible bulk porous materials, see Figs. 3, 4, and 5.

(6) Experimental characteristics of normal impedance and absorption coefficient in the frequency range 300 to 3000 Hz have been established for two types of Kevlar 29 porous blanket, see Table I.

(7) Acoustic parameters based on the theory of Zwikker and Kosten for Kevlar and Scottfoam have been established, see Table I.

(8) Agreement between measured and predicted values of impedance and absorption coefficient based on bulk properties is satisfactory. The wave motion was assumed to be decoupled but it appears that some coupling effects are in evidence, see Figs. 6-12.

B. Recommendations

(1) No concerted effort to refine the characterization of porous, flexible blankets for critical applications has been made. That might involve preparing a set of parametric curves and procedures based on coupled wave motion. If Kevlar or Scottfoam or any other porous, flexible blanket type material becomes a candidate material for duct liners then such an effort may be warranted. This also may be an essential procedure if effects of extended wave reaction on impedance of porous, bulk duct liners is to be understood and predicted.

(2) If angle of incidence effects on impedance and absorption of duct liners or other porous materials are to be fully predicted then a comprehensive theory based on a three-dimensional wave model is required. Once the essential parameters have been established then wave coupling can be introduced and its effect on the surface characteristics predicted probably via numerical analysis.

(3) Effects of finite sample size are not included in the theory of Zwicker and Kosten as applied to the testing of bulk materials in an impedance tube. Therefore, measured values of impedance and absorption can differ in detail from predicted values even if the acoustic parameters are essentially correct. Such discrepancies have been noted in work by others⁽¹⁵⁾ and similar discrepancies also were found here for some samples. For example, if the samples of high ϕ Kevlar are not mounted firmly in the holder and held by compressional forces they will vibrate and resonate at particular frequencies by virtue of their finite diameter. This is evidenced by extreme changes in impedance over fairly narrow frequency ranges which are not predicted by theory in detail. Even with precautions, samples of Kevlar exhibited some irregular behavior as noted in experimental values, see Figs. 8, 9, and 12.

(4) The elastic bulk modulus κ_s must be carefully defined and measureable if accurate information about wave speeds, wave coupling action, and extended reaction effects in porous materials is required. Good definitions, methods of prediction and measurements of all parameters is a goal worthy of further study.

(5) The theory of Zwicker and Kosten can be used to characterize the acoustical impedance of porous ground. If characterized properly such information could be used to predict "excess" attenuation of sound attributed to absorption and reflection in applications such as aircraft fly-over noise, freeway traffic noise, the certification of noise sources, industrial plant site noise, and a host of other community noise prediction methods. This

effort might require both an extensive experimental as well as theoretical study to establish the appropriate characterization.

APPENDIX A

CONCEPTS OF EQUIVALENT DENSITY AND DYNAMIC RESISTANCE FOR POROUS MATERIALS

The purpose of this work is to derive expressions for the equivalent density ρ_e and the dynamic resistance Φ_e applicable to flexible, highly porous blankets and rigid, highly porous tile. These are extreme cases that can be handled on the basis of the analysis of Zwicker and Kosten.

The proper procedure is to examine expressions for the wave propagation constant Γ in cases where wave coupling is significant and then endeavor to express it in the form

$$\Gamma_e^2 = \frac{\omega^2}{c_e^2} \left(1 + i \frac{\Phi_e}{\omega \rho_e} \right) \quad A-1$$

which is valid for decoupled motion where $c_e^2 = (\kappa_a \rho_e \Omega)^{-1}$

In order to do this in a systematic way one invokes the inequality

$$\kappa_{12} S_{21} \sigma_{22} + \frac{\Omega}{1 - \Omega} \kappa_{21} S_{12} \sigma_{11} \ll \kappa_{11} \sigma_{22} S_{22} + \frac{\Omega}{1 - \Omega} \kappa_{22} \sigma_{11} S_{11} \quad A-2$$

which easily holds for highly porous materials, i.e. $\Omega \geq 0.9$, having a structure constant $k_s \leq 4$ for all frequencies of interest, see Eq. 13. Also, the value of the stiffness ratio $\Omega \kappa_s / \kappa_a$ is not critical here so that A-2 is valid for both extremes namely $\Omega \kappa_s / \kappa_a \gg 1$ and $\Omega \kappa_s / \kappa_a \ll 1$.

By writing the expression for Γ , Eq. 11, in the form

$$\Gamma_e^4 - b \Gamma_e^2 + c = 0 \quad A-3$$

one finds after invoking A-2 that

$$b = \frac{\omega^2}{c_a^2} \left[\left(\kappa_{11} + \frac{K_{sa}}{\tau_{sa}} \right) + i \left(\frac{\kappa_{11} + K_{sa}}{\tau_{sa}} \right) \frac{1}{Q_{es}} \right] \quad A-4$$

where

$$K_{sa} \equiv \Omega \kappa_s / \kappa_a$$

$$\tau_{sa} \equiv \rho_a / \rho_{es}$$

and

$$c_a^2 \equiv (\kappa_a \Omega \rho_a)^{-1}$$

Also one finds that

$$c \approx \omega^2 \Omega^3 \kappa_s \kappa_a \phi^2 \left[(Q_{es} + i)(Q_a + i) - (Q_{ei} + i)^2 \right] \quad A-5$$

where the Q's have been defined in the text.

On the assumption that $Q_{ei}^2 \ll 1$ at all frequencies of interest the ratio c/b becomes

$$\frac{c}{b} \approx \frac{\omega^2}{c_s^2 (\kappa_{11} + K_{sa}/\tau_{sa})} \left[\frac{1 + i \mu_{sa}/\tau_{sa}}{1 + i \sigma_{sa}/(\kappa_{11} + K_{sa}/\tau_{sa})} \right] \quad A-6$$

where

$$\mu_{sa} = (1 + \tau_{sa})/Q_{es}$$

and

$$\sigma_{sa} = \left(\frac{\kappa_{11} + K_{sa}}{\tau_{sa}} \right) / \frac{1}{Q_{es}}$$

$$c_s^2 \equiv (\kappa_s \rho_{es} \Omega^2)^{-1}$$

Note, if $\kappa_s = 1$, then $Q_{ei} \equiv 0$ and there is no inertial coupling.

For flexible, porous blankets, $\tau_{sa} \ll 1$ and

$$K_{sa} = \Omega \kappa_s / \kappa_a \gg \kappa_{11} = 1 + \left(\frac{1 - \Omega}{\Omega} \right)^2 \left(\frac{\Omega \kappa_s}{\kappa_a} \right) (1 - P_0 \kappa_a)$$

which reduces to

$$\left(\frac{1 - \Omega}{\Omega} \right)^2 (1 - \kappa_a P_0) \ll 1$$

an inequality that is almost identical with the inequality in Eq. 13 and hence easily satisfied. Thus, from A-1

$$\Gamma_e^2 \approx \frac{c}{b} \approx \frac{\omega^2}{c_e^2} (1 + i \phi_e / \omega \rho_e) \quad A-7$$

where

$$c_e^2 = c_s^2 (\kappa_{11} + K_{sa} / \tau_{sa}) \quad a)$$

and

$$\rho_e = \rho_a \left(1 + \frac{\rho_{es}}{\rho_a} \frac{1}{Q_{es}^2 + 1} \right) \quad b)$$

A-8

$$\phi_e = \phi \left(\frac{Q_{es}^2}{Q_{es}^2 + 1} \right) \left(1 + 2 \frac{\rho_a}{\rho_{es}} \right) \approx \phi \left(\frac{Q_{es}^2}{Q_{es}^2 + 1} \right) c)$$

since $\rho_a / \rho_{es} \ll 1$.

At high frequencies, $\frac{\rho_a}{\rho_{es}} Q_{es}^2 \gg 1$ and $\rho_e \approx \rho_a$ while at low frequencies, i.e. $Q_{es}^2 \ll 1$, the effective density of air in the pores of the material is $\rho_a + \rho_{es}$ indicating that the motion of the air particles and the fibers are tightly coupled together and move as one entity.

It also is interesting to note that an equivalent quality factor Q_e can be defined as

$$Q_e \equiv \frac{\omega \rho_e}{\phi_e} = Q_a \left(1 + \frac{\rho_{es}}{\rho_a} \frac{1}{Q_{es}^2} \right) \quad A-9$$

which can be approximated by Q_a only on the added assumption that

$Q_{es}^2 \gg \rho_{es} / \rho_a$. This implies that any empirical analysis based upon a single descriptor like Q_a must be justified carefully and likely to have limited applicability especially with regard to frequency range, most likely high frequencies.

At low frequencies $\phi_e \approx \phi Q_{es}^2$ for flexible, porous blankets indicating that the dynamic resistance is very low and varies with the square of the frequency while at high frequencies, where $Q_{es}^2 \gg 1$,

ϕ_e becomes identical with the specific air flow resistance ϕ since no energy dissipation in the fibers has been taken into account. This result does not imply that ϕ is always independent of frequency, however. These formulas agree fairly well with Beranek's expressions⁽⁴⁾ if $\rho_e \Omega$ replaces the equivalent density $\langle \rho_1 \rangle$ in his work.

The other extreme where $K_{sa} \ll 1$ obtains for rigid porous tile or rigid fibrous boards. In that case

$$\Gamma_e^2 \approx b = \frac{\omega^2}{c_a^2} \left(\frac{\kappa_{11} \tau_{sa} + K_{sa}}{\tau_{sa}} \right) \left[1 + i \frac{\kappa_{11} + K_{sa}}{\kappa_{11} \tau_{sa} + K_{sa}} \frac{1}{Q_{es}} \right] \quad A-10$$

which is of the desired form. One then readily identifies

$$\rho_e = \rho_a \left(\kappa_{11} + K_{sa} / \tau_{sa} \right)$$

or

$$\frac{\rho_e}{\rho_a} = \kappa_{11} + \left(\frac{\Omega \kappa_s}{\kappa_a} \right) \left(\frac{\rho_{es}}{\rho_a} \right) \quad A-11$$

which is a ratio that is sometimes called a structure factor and probably fairly independent of frequency. This result was verified by Beranek for

wire screen mesh but not for commercial tiles due to their inherent inhomogeneity. However, the behavior of κ_s with frequency for rigid tile materials and rigid fibrous board is not known. If the air motion is isothermal (at very low frequencies)

$$\rho_e \approx \rho_0 \kappa_s / \Omega$$

for $\Omega \approx 1$ and $\kappa_s \leq 4$ independent of the value of κ_s . Thus at low frequencies $\rho_e \approx \rho_a$ the apparent density of the air of the pores. Hence, the frequency behavior of ρ_e for flexible blankets and rigid board is quite different.

The equivalent dynamic resistance for rigid board is

$$\Phi_e = \Phi \left(\kappa_{11} + \frac{\Omega \kappa_s}{\kappa_a} \right) \quad \text{A-12}$$

There is no apparent frequency variation in Φ_e for rigid board either. The second term $\Omega \kappa_s / \kappa_a < \kappa_{11}$ at all frequencies. However, Beranek found that Φ_e decreased with frequency at sufficiently high frequencies for reasons unknown. At low frequencies he showed experimentally that $\Phi_e \approx \Phi$ for fine wire mesh screen. This suggests that Eq. A-12 is a low frequency formula and hence not valid over a wide range of frequencies. It might be concluded that rigid screens can become acoustically flexible at high frequencies and are stiff only at low frequencies. This matter bears more careful study and perhaps a reformulation of the dynamical equations of motion is in order to account for material stiffness. One possibility based on a casual observation of cross coupling terms in Eq. 10 is that no dynamic stiffness cross coupling terms appear, i.e. $\sigma_{12} = \sigma_{21} = 0$ in the coupling matrix. Perhaps such coupling

terms should be included in order to develop a more complete theory applicable to a wide variety of porous materials and valid over wide ranges of frequency. The theory as developed by Zwikker and Kosten does appear, therefore, to be applicable to highly porous, flexible materials and rigid porous materials over a limited range of frequencies. Hence, it has limited applicability in so far as engineering design of materials is concerned. One would desire to be able to predict both the real and imaginary parts of $Z_a/\rho_0 c_0$ and specify them in terms of material parameters at all frequencies of concern.

In the theory of Zwikker and Kosten knowledge of the frequency behavior of $\Omega\kappa_s/\kappa_a$ appears essential and should not be limited to predictions of upper and lower bounds. This is an area that deserves more study.

Finally, Eq. A-1 as here formulated could provide the basis for a more systematic parametric analysis of a wide range of porous materials including flexible blankets, ground cover, and stiff tile. This also is an area that deserves more study. For example, it is not known whether the inequality of A-2 is valid for various types of porous ground but it appears to be easily satisfied for a wide variety of commercial materials designed as good absorbers.

APPENDIX B

FUNDAMENTAL EQUATIONS OF MOTION

In this appendix the fundamental equations of Zwikker and Kosten⁽²⁾ will be recast into the form employed in the text of their report. In an elastic porous solid containing air the equations of motion in the elastic frame are given as

$$-\frac{\partial p_1}{\partial x} = \rho_1 \frac{\partial v_1}{\partial t} + s (v_1 - v_2) \quad a)$$

and

$$-\frac{\partial p_1}{\partial t} = K_1 \frac{\partial v_1}{\partial x} - \frac{(1-h)}{h} \frac{\partial p_2}{\partial t} \quad b)$$

and in the air of the pore space as

B-1

$$-\frac{\partial p_2}{\partial x} = \rho_2 \frac{\partial v_2}{\partial t} + s (v_2 - v_1) \quad c)$$

and

$$-\frac{\partial p_2}{\partial t} = h K_2 \frac{\partial v_2}{\partial x} + (1-h) (K_2 - P_0) \frac{\partial v_1}{\partial x} \quad d)$$

where the parameters ρ_1 , ρ_2 , K_1 , K_2 , h and s are defined on page 52 in Zwikker and Kosten. In their work p_1 is the force per unit area of cross-section of the sample acting as the frame, v_1 is the mean velocity of the frame, p_2 is the excess force per unit area of cross-section of the sample acting on the air, and v_2 is the mean velocity of the air in the frame.

For convenience the Eqs. of B-1 are recast in operational notation as

$$-\frac{\partial p_1}{\partial x} = \{[\rho_1 + \rho_2(k_s - 1)] \frac{\partial}{\partial t} + h^2 \sigma\} v_1 - [\rho_2(k_s - 1) \frac{\partial}{\partial t} + h^2 \sigma] v_2 \quad a)$$

B-2

$$-\frac{\partial p_1}{\partial t} = [K_1 + (1-h)^2 (K_2 - P_0)] \frac{\partial v_1}{\partial x} + (1-h) K_2 \frac{\partial v_2}{\partial x} \quad b)$$

$$-\frac{\partial p_2}{\partial t} = (\rho_2 k_s \frac{\partial}{\partial t} + h^2 \sigma) v_2 - [\rho_2(k_s - 1) \frac{\partial}{\partial t} + h^2 \sigma] v_1 \quad c)$$

$$-\frac{\partial p_2}{\partial t} = h k_2 \frac{\partial v_2}{\partial t} + (1 - h) (k_2 - p_0) \frac{\partial v_1}{\partial x} \quad d)$$

after substituting for the coupling coefficient s .

In order to write the parameters and variables in a more common notation define:

$$\begin{aligned} h &= \Omega & \sigma &= \Phi \\ p_1 &= (1 - \Omega) p_s & \rho_1 &= (1 - \Omega) \rho_s \\ p_2 &= \Omega p_a & \rho_2 &= \Omega \rho_0 \\ v_2 &= 1/\Omega v_a & k_2 &= 1/\kappa_a \\ v_1 &= v_s & k_1 &= 1/\kappa_s \end{aligned} \quad B-3$$

Here p_s is interpreted as the dynamic pressure of the solid frame, p_a is the acoustic excess pressure in the air pores, v_s is the mean velocity of the frame, and v_a is the particle velocity of the sound waves in the air pores.

By assuming harmonic excitation at an angular frequency ω and propagation of elastic and sound waves in the x -direction according to the convention $\exp [-i(\Gamma x - \omega t)]$ Eq. B-2 can be expressed as

$$\frac{1 - \Omega}{\Omega} \Gamma p_s = \Omega (\omega \rho_{es} + i \Phi) v_s - (\omega \rho_{ei} + i \Phi) v_a \quad a)$$

$$\omega \kappa_s (1 - \Omega) p_s = \kappa_{11} \Gamma v_s + \kappa_{12} \Gamma v_a \quad b)$$

B-4

$$\Gamma p_a = (\omega \rho_a + i \Phi) v_a - \Omega (\omega \rho_{ei} + i \Phi) v_s \quad c)$$

and

$$\omega \kappa_a \Omega p_a = \kappa_{22} \Gamma v_a + \kappa_{21} \Gamma v_s \quad d)$$

where P_s , P_a , V_s and V_a are complex amplitudes and the parameters

Φ , ρ_{es} , ρ_{ei} , ρ_a , κ_{11} , κ_{12} , κ_{22} , and κ_{21} are defined in the text.

It is worthwhile noting that Eqs. B-1 (b) and (d), the equations of continuity, have been criticized and reformulated on various grounds⁽¹⁷⁾.

Also, the definitions of p_1 and p_2 render these equations invalid⁽¹⁸⁾.

The upshot of this matter is to simply remove the term $P_o \kappa_a$ from the dilatational coefficients κ_{11} and κ_{21} in Eqs. 5b and 6b of the text.

However, for highly porous frames considered in this report this procedure does not appear to be a significant change and it was decided to leave the definitions of Zwikker and Kosten intact. If the basic equations are reformulated for precision design purposes then such refinements may be warranted.

Material Parameter	Kevlar 29 low Φ Type	Kevlar 29 high Φ Type	Scottfoam open-cell Type
Φ (cgs rayls)	46.4	79.4	18
k_s	2.1	3.2	2.1
Ω	.940	.938	.950
k_a high frequency value	$\frac{1}{p_o}$	$\frac{1}{p_o \gamma}$	$\frac{1}{p_o}$
ρ_s (g/cm ³)	1.44	1.44	0.60
ρ_{es}/ρ_a	38	25	13
d(cm.)	1.3×10^{-3}	1.3×10^{-3}	2.1×10^{-3}

Table I. Mechanical and Acoustic Parameters of Test Samples.

FIGURE LEGEND

- Figure 1. Plots of the normalized propagation constant $\frac{c_a}{\omega} \Gamma_a = B + iA$ versus Q_{es} for Kevlar 29 based on $\rho_{es}/\rho_a = 38$. The subscript 1 refers to coupled wave motion and the subscript 2 refers to decoupled wave motion.
- Figure 2a. Plot of the normalized resistance $R_a/\rho_0 c_0$ for low Φ Kevlar 29 based on $\rho_{es}/\rho_a = 38$ and $\sqrt{k}/\Omega = 1.3$. The subscript 1 refers to coupled wave motion and the subscript 2 refers to decoupled motion.
- Figure 2b. Plot of the normalized reactance $-X_a/\rho_0 c_0$ for low Φ Kevlar 29 based on $\rho_{es}/\rho_a = 38$ and $\sqrt{k}/\Omega = 1.3$. The subscript 1 refers to couple wave motion and the subscript 2 referes to decoupled motion.
- Figure 3. Plot of $R_a/\rho_0 c_0$ versus Q_a employing \sqrt{k}/Ω as a parameter for decoupled motion.
- Figure 4. Plot of $-X_a/\rho_0 c_0$ versus Q_a employing \sqrt{k}/Ω as a parameter for decoupled motion.
- Figure 5. Plot of normal incidence sound absorption coefficient α_a versus Q_a employing \sqrt{k}/Ω as a parameter for decoupled motion.
- Figure 6. Plots of $R_a/\rho_0 c_0$ versus Q_a for low Φ Kevlar based on parameters in Table I. Adiabatic bulk modulus is shown for high frequencies. Experimental data shown for frequency range from 300 to 3000 Hz.
- Figure 7. Plot of $-X_a/\rho_0 c_0$ versus Q_a for low Φ Kevlar based on parameters in Table I. Experimental data shown for frequency range from 300 to 3000 Hz.
- Figure 8. Plot of $R_a/\rho_0 c_0$ versus Q_a for high Φ Kevlar based on data in Table I.
- Figure 9. Plot of $-X_a/\rho_0 c_0$ versus Q_a for high Φ Kevlar based on parameters in Table I.
- Figure 10. Plot of $R_a/\rho_0 c_0$ versus Q_a for Scottfoam based on parameters in Table I. Experimental data for frequency range from 500 to 3500 Hz.
- Figure 11. Plot of $-X_a/\rho_0 c_0$ versus Q_a for Scottfoam based on parameters in Table I.
- Figure 12. Normal incidence sound absorption characteristics for Scottfoam, low Φ Kevlar 29, and high Φ Kevlar 29.

REFERENCES

1. Scott, R. A.: Proc. Phys. Soc. 58, 165-183, (1946)
2. Zwikker, C. and Kosten, C. W.: Sound Absorbent Materials, Elsevier Publishing Co., Inc., New York, 1949.
3. Morse, P. M. and Bolt, R. H., Revs. Mod. Phys. 16, 69-150 (1944).
4. Beranek, L. L.: J. Acoust. Society of America, 19, 556-568, (1947).
5. Morse, R. W.: J. Acoust. Society of America, 24, 696-700 (1952).
6. Smith, C. D. and Parrott, T. L.: NASA Tech. Memo. 78654, NASA Langley Research Center, Jan. 1978.
7. Hersh, A. S. and Walker, B.: "Acoustic Behavior of A Fibrous Bulk Material", AIAA Paper 75-0599, 5th Conference on Aeroacoustics, Seattle, WA, March 1979.
8. Smith, C. D.: "Comparative Studies of Methods of Measuring Acoustic Properties of Porous Materials" Thesis submitted to the faculty of George Washington University in partial fulfillment of requirement for M.S. in Acoustics, 1979.
9. Morse, P. M. and Ingard, K. V.: Theoretical Acoustics, McGraw Hill Publishing Company, Inc., 1968.
10. Kosten, C. W. and Janssen, J. H.: Acoustica 7, 372-378, (1957).
11. McGrath, J. W.: J. Acoust. Soc. of America, 24, 305-309, (1952).
12. Delany, M. E. and Bazley, E. W.: Applied Acoustics 3, 105-116, (1970).
13. Chase, D. M.: J. Acoust. Soc. Am., 65, 1-8 (1979).
14. Mechel, F. P.: Acoustica 35, 209-213, (1976).
15. Beranek, L. L.: J. Acoust. Soc. Am. 19, 420-427, (1947).
16. Piercy, J. E. and Embleton, T. F. W.: "Excess Attenuation and Impedance of Common Ground Surfaces Characterized by Flow Resistance", Paper X-1 50th Anniversary Celebration Meeting, Acoust. Soc. Am. Boston, Mass, June 11-15, 1979. See also Embleton, Piercy, and Olson, J. Acoustic. Soc. Am. 59 267-277, (1976).
17. Rosin, G. S., Societ Physics, 9 60-64, (1973).
18. Zarek, J. H. B., J. Sound Sound Vib., 61, 205-234, (1978).

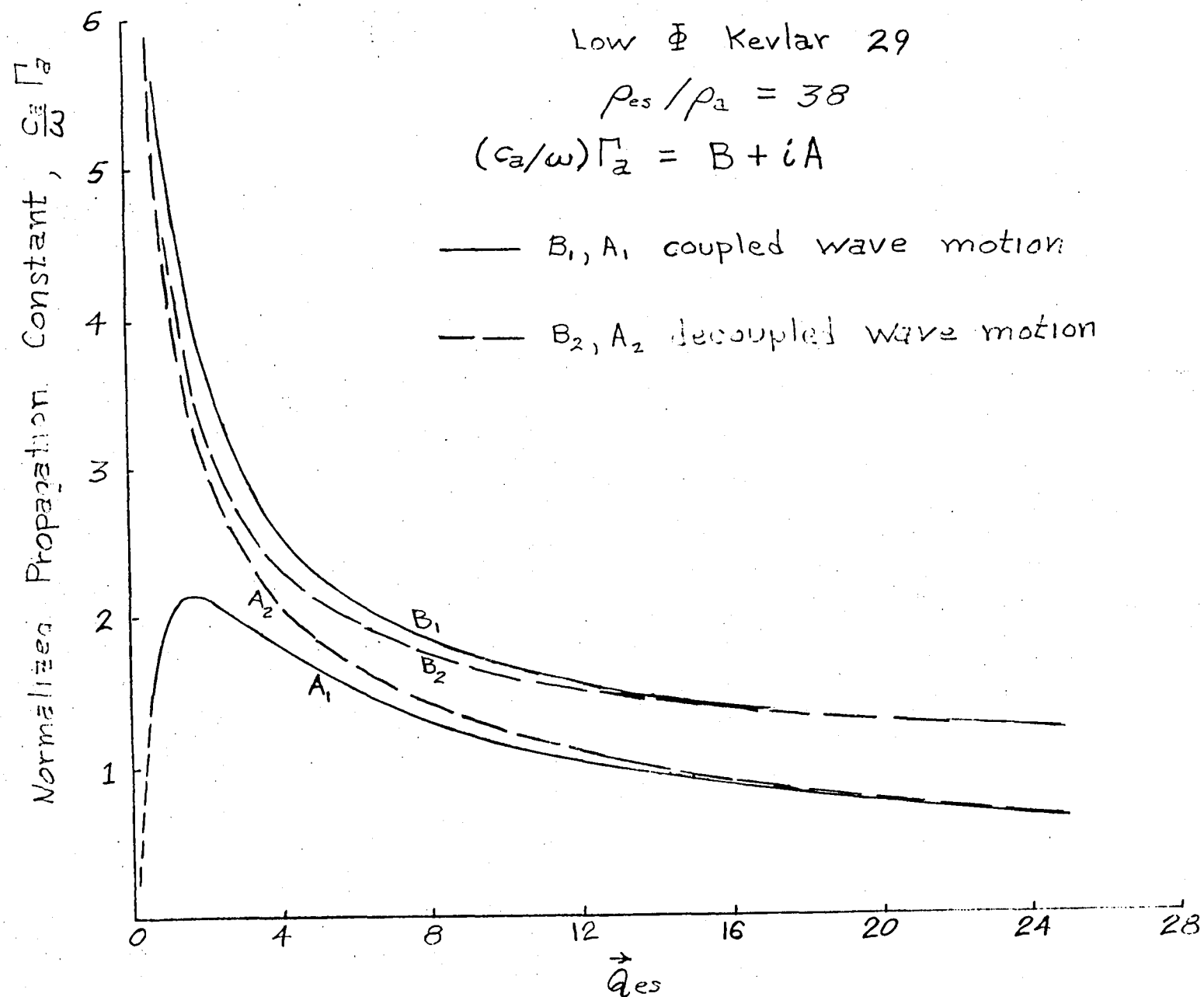


Figure 1.- Normalized acoustic propagation constant for Kevlar 29.

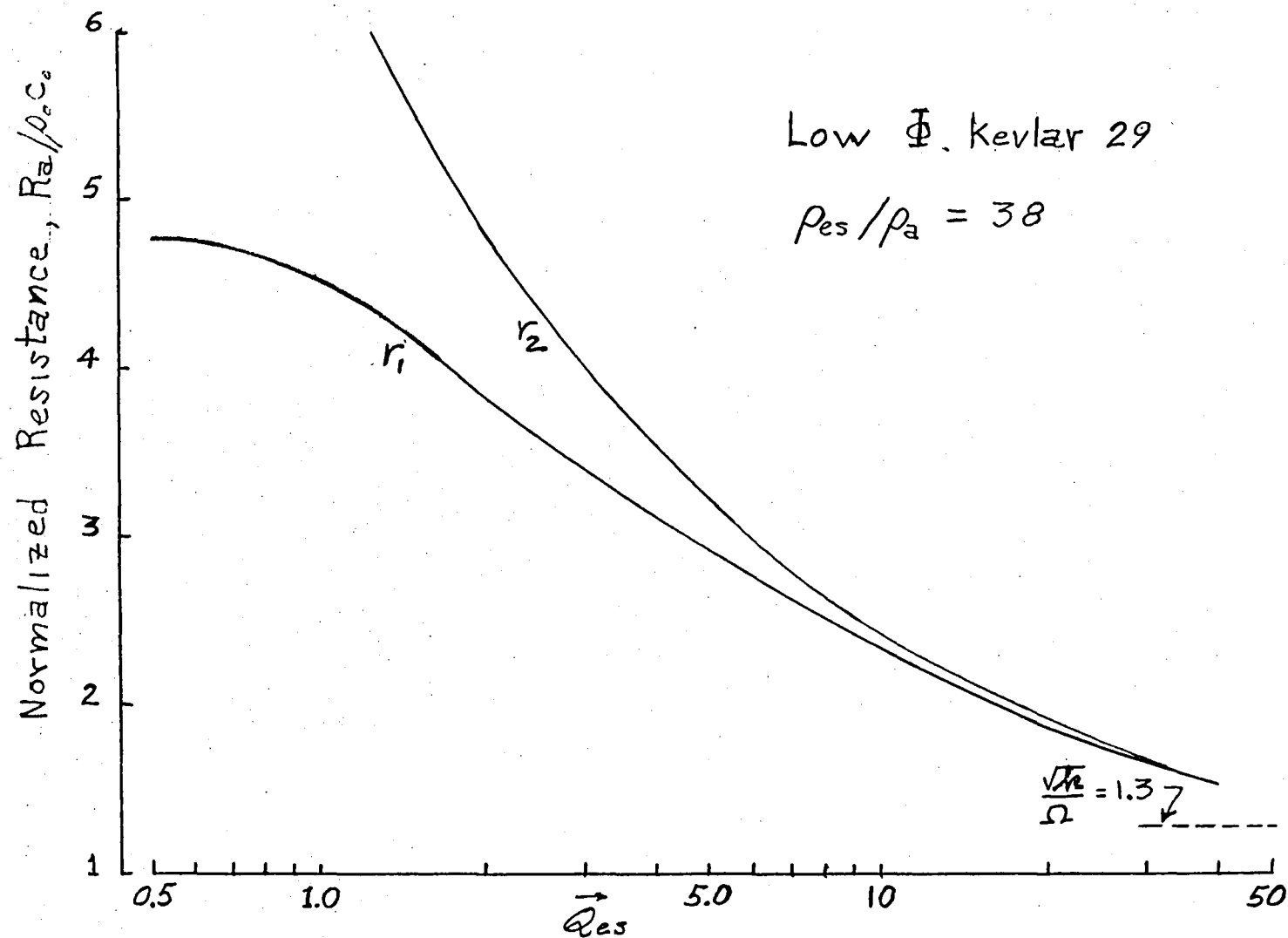


Figure 2a.- Normalized acoustic resistance for Kevlar 29, r_1 - coupled motion, r_2 - decoupled motion.

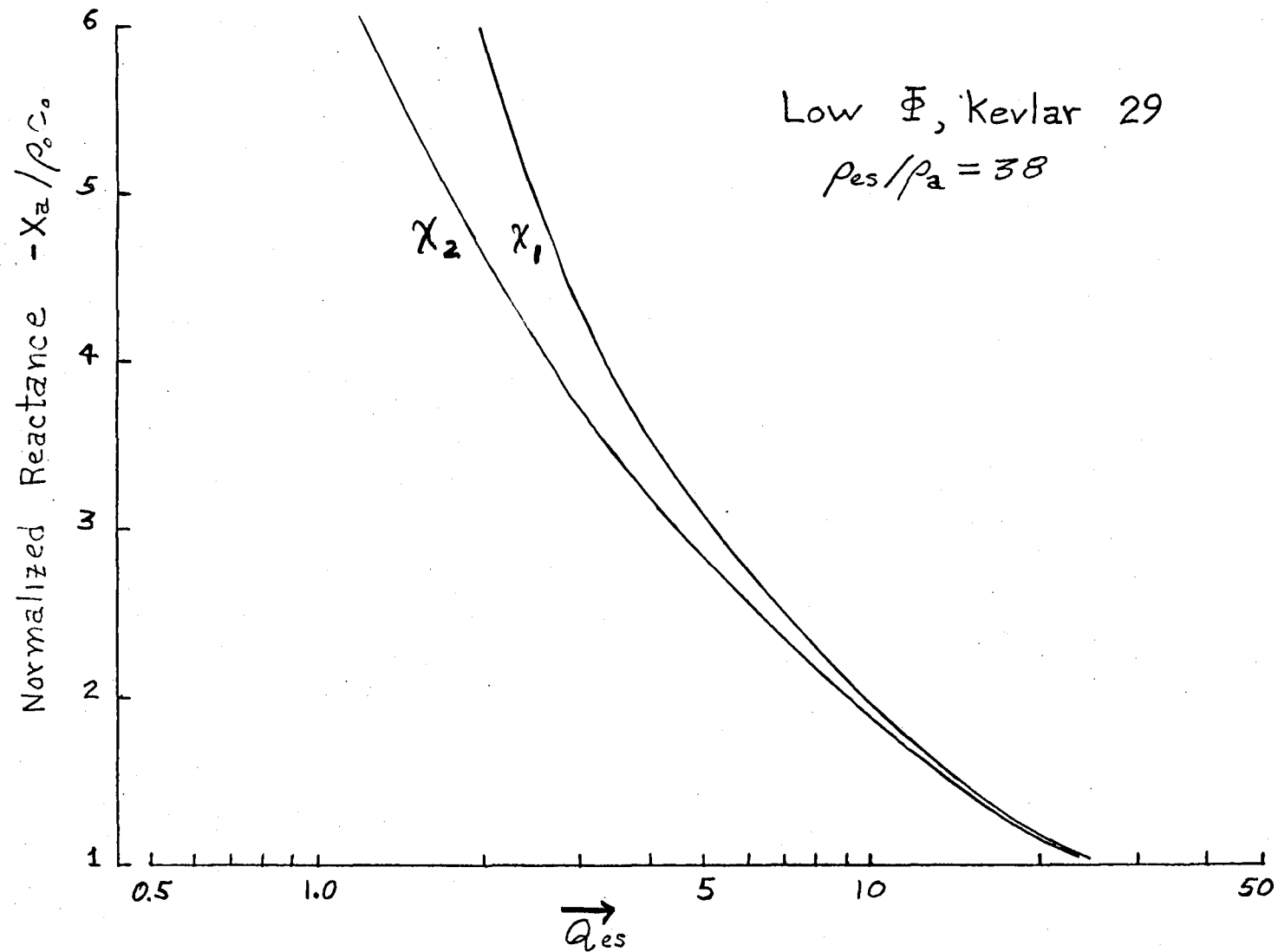


Figure 2b. Normalized acoustic reactance for Kevlar 29, x_1 - coupled motion, x_2 - decoupled motion.

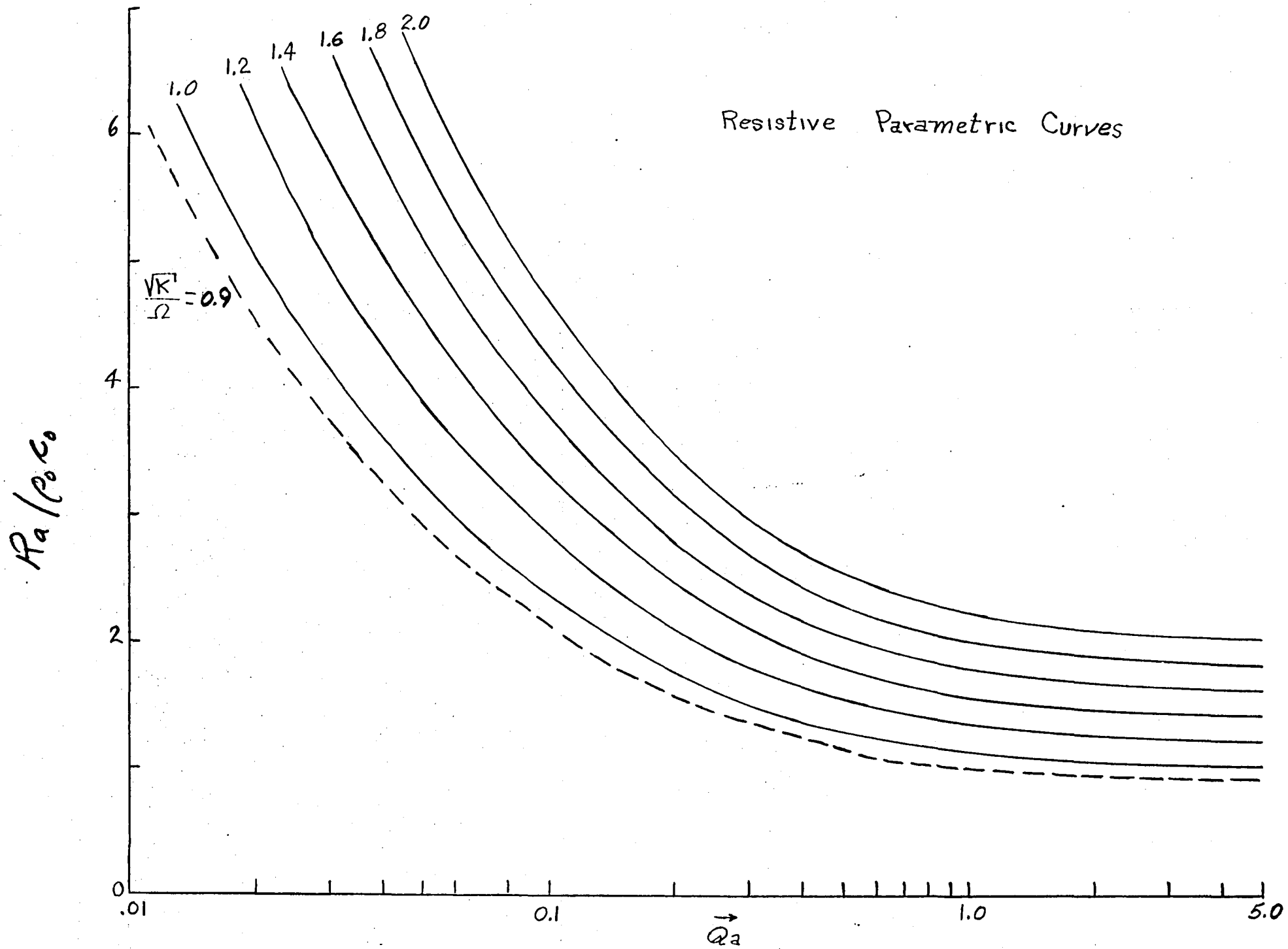


Figure 3.- Resistive parametric curves for decoupled wave motion.

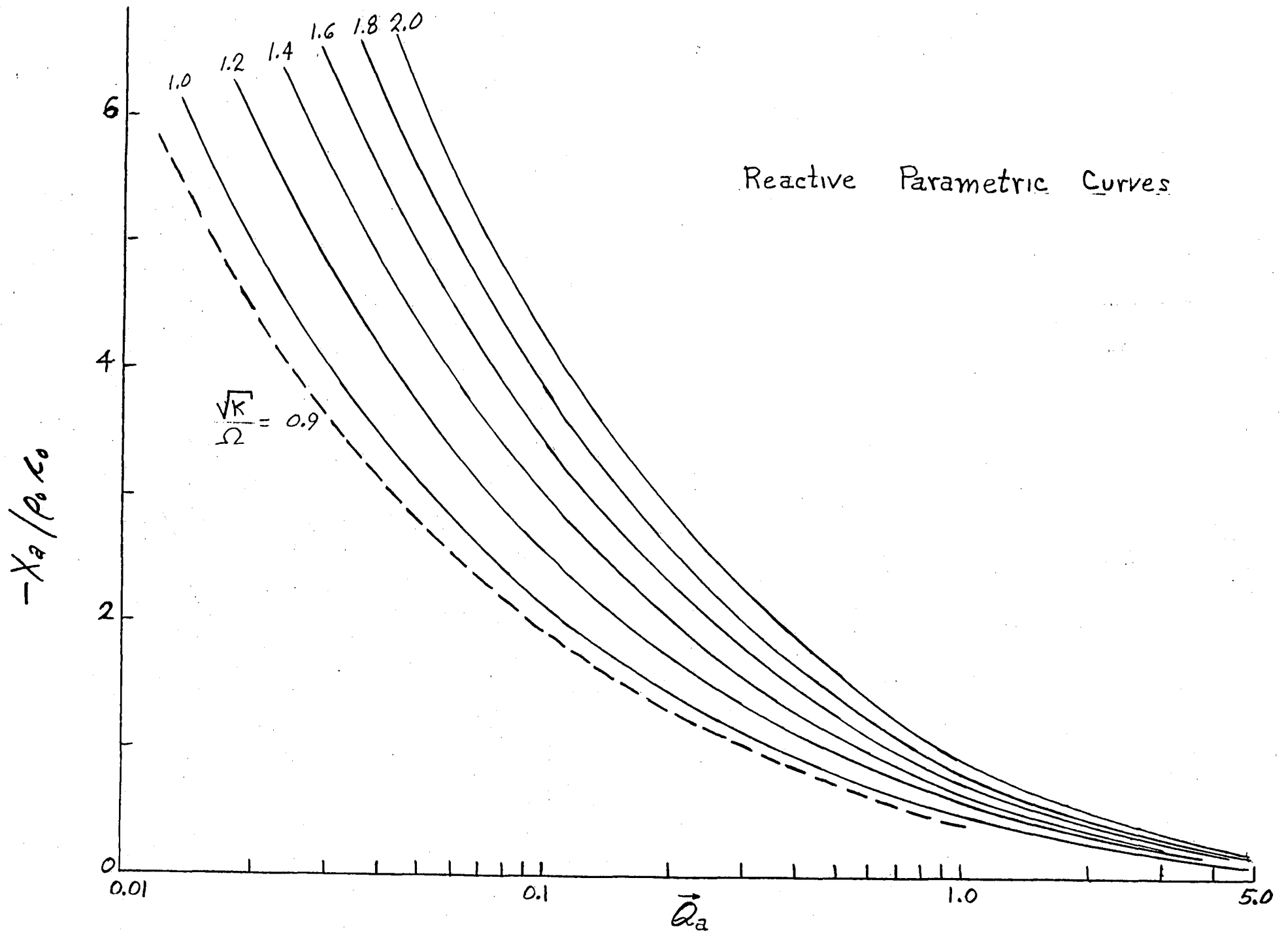


Figure 4.- Reactive parametric curves for decoupled wave motion.

Absorption Coefficient Parametric Curves

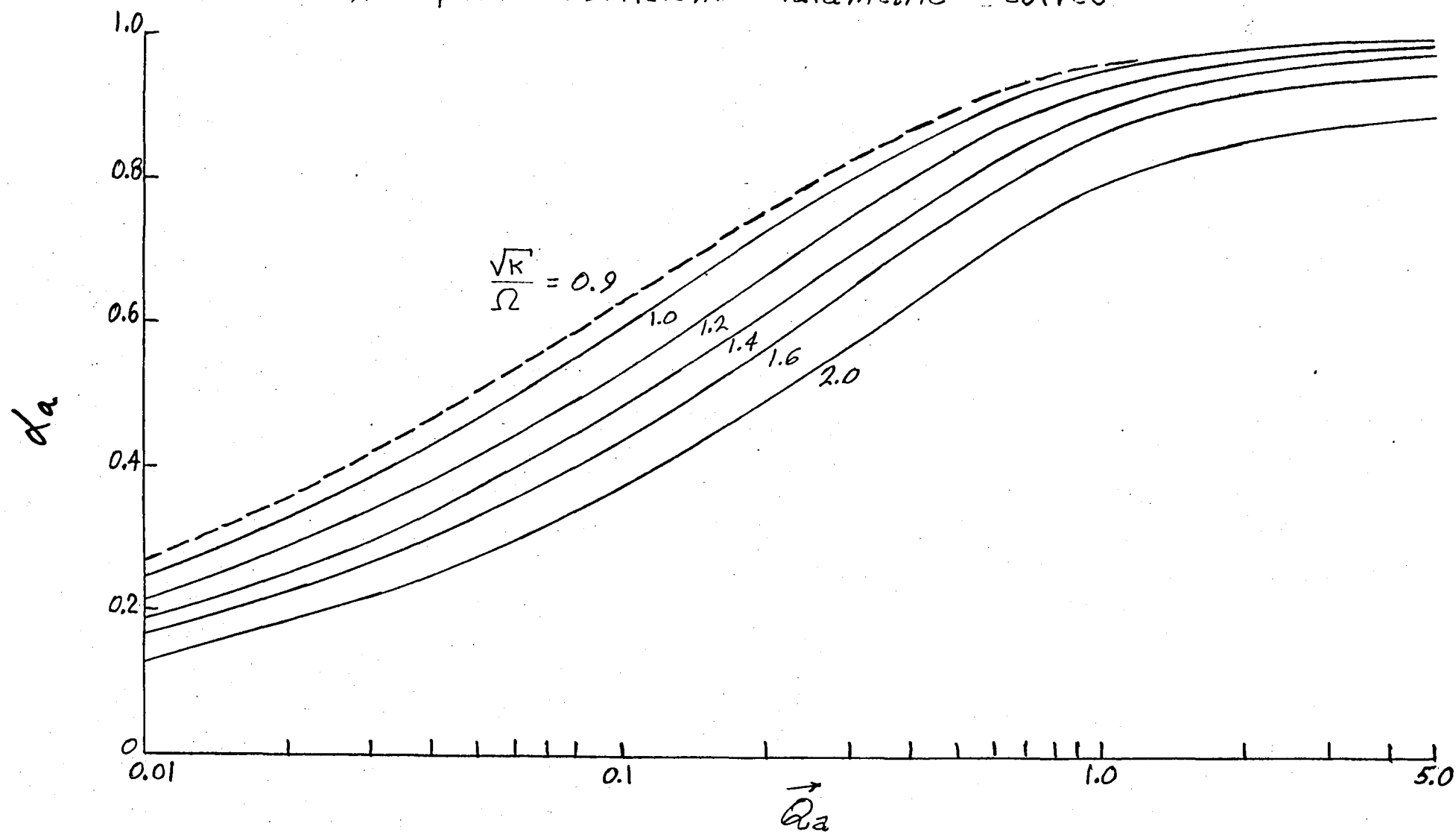


Figure 5.- Absorption parametric curves for decoupled wave motion.

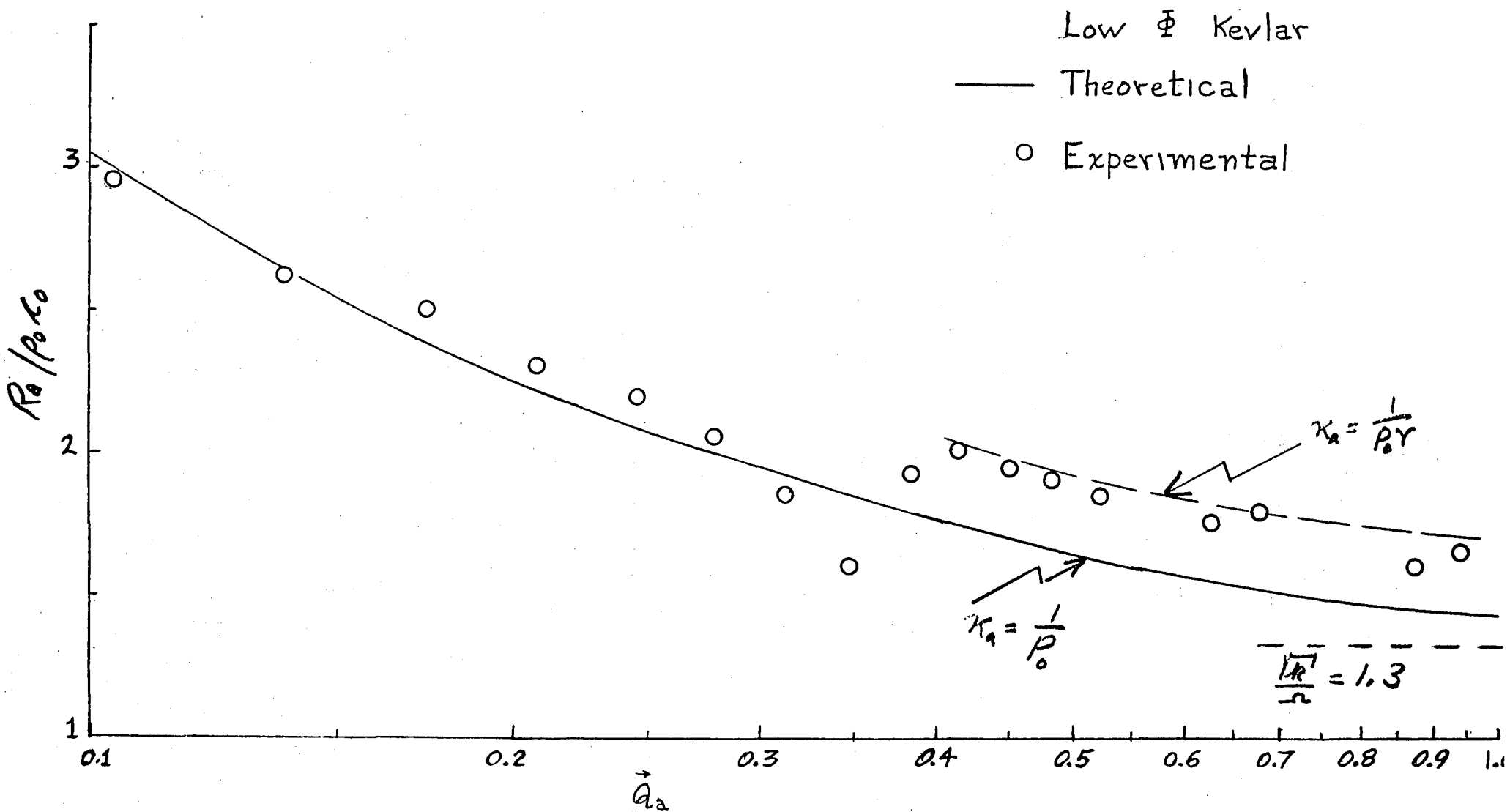


Figure 6.- Comparisons of the normalized acoustic resistance for low Φ Kevlar sample.

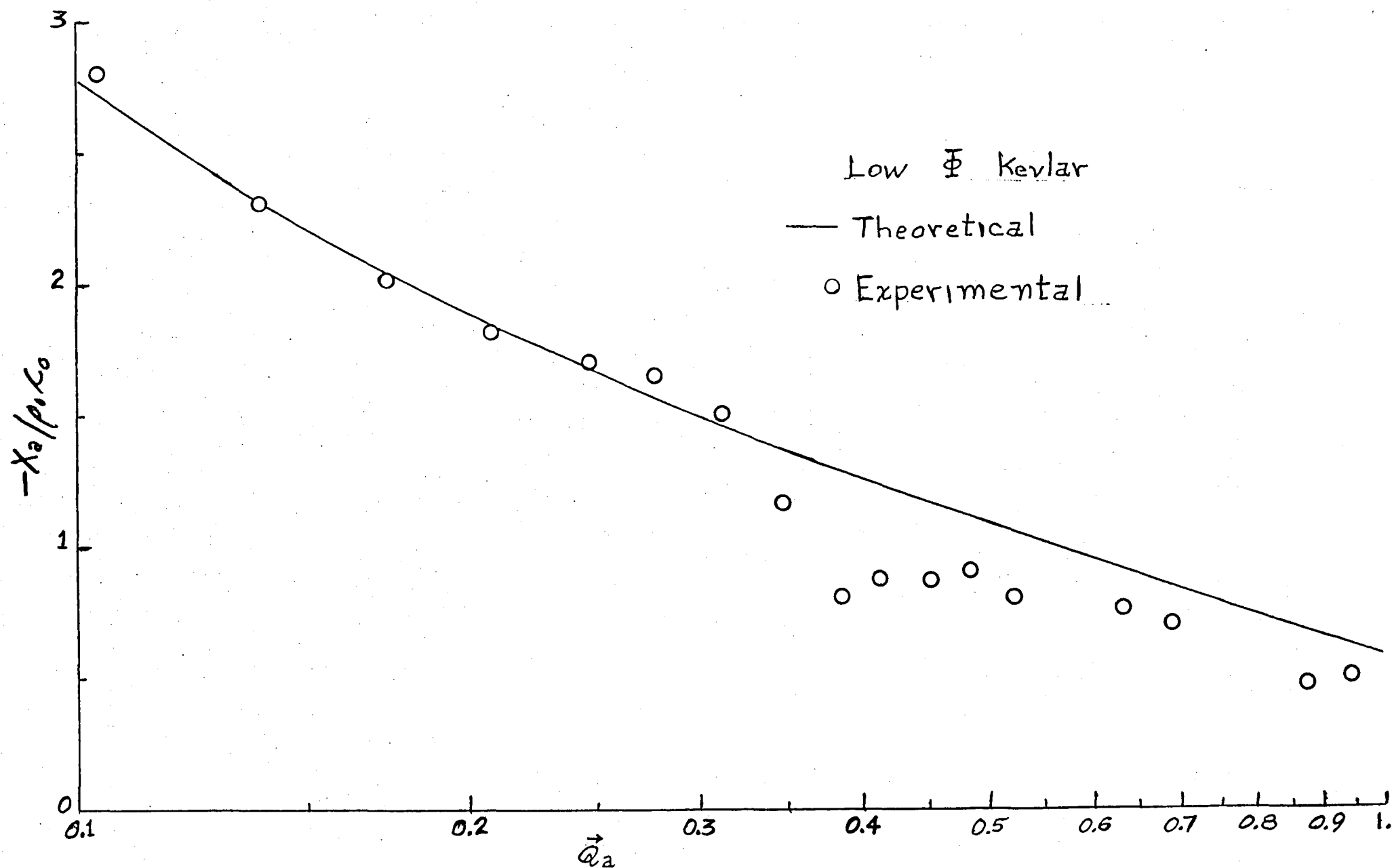


Figure 7.- Comparisons of the normalized acoustic reactance for low Φ Kevlar sample.

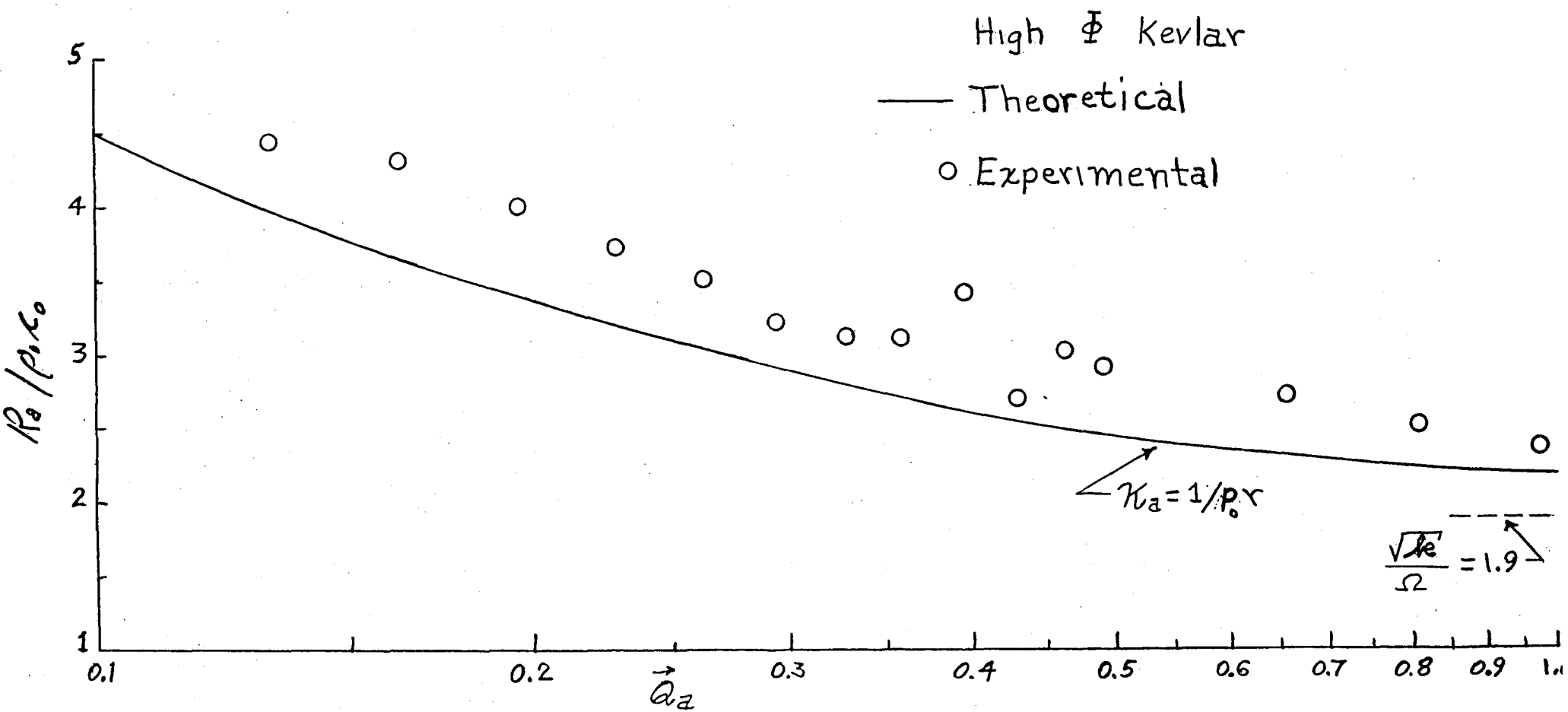


Figure 8.- Comparisons of the normalized acoustic resistance for high Φ Kevlar sample.

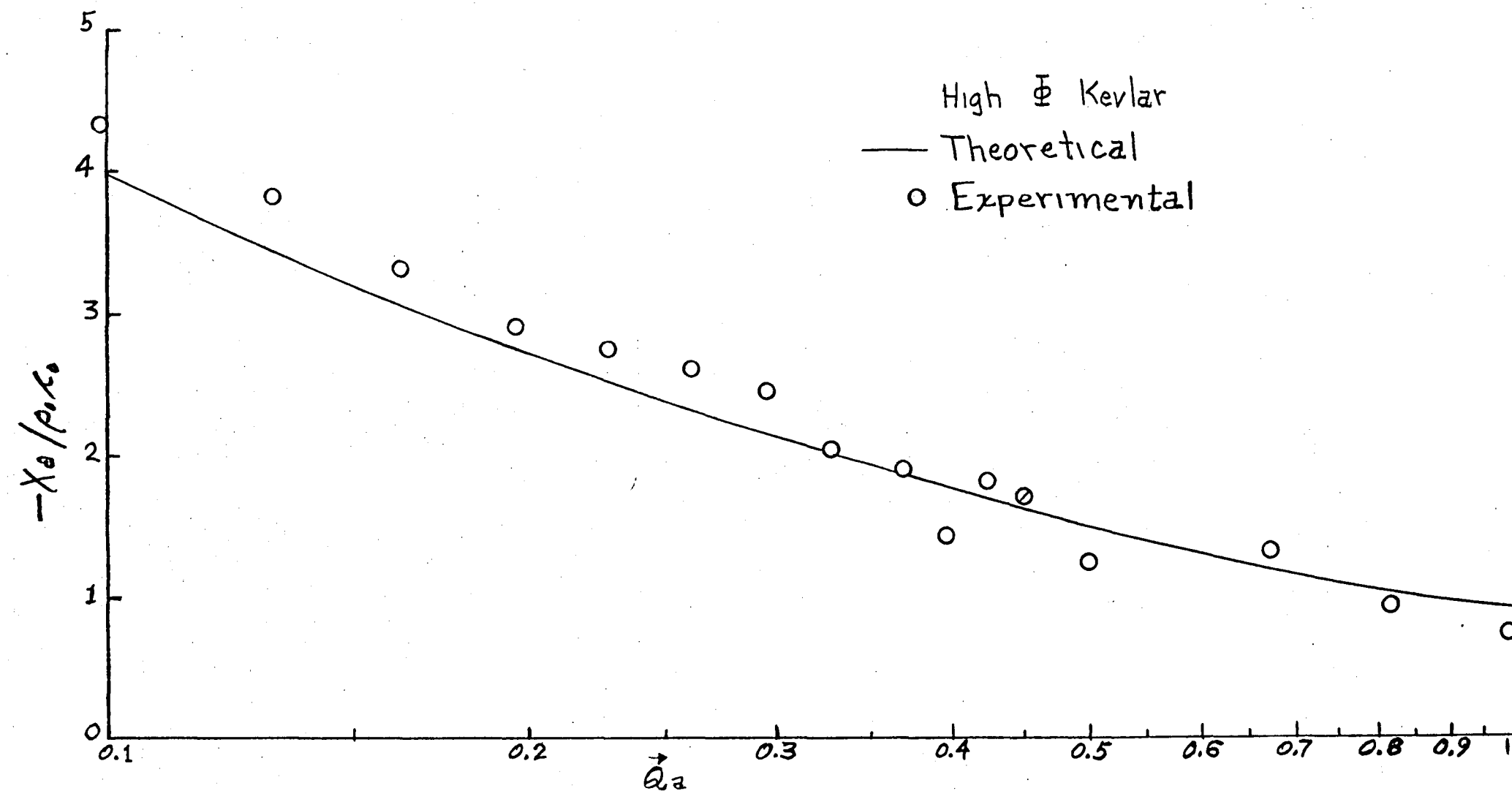


Figure 9.- Comparisons of the normalized acoustic reactance for high Φ Kevlar sample.

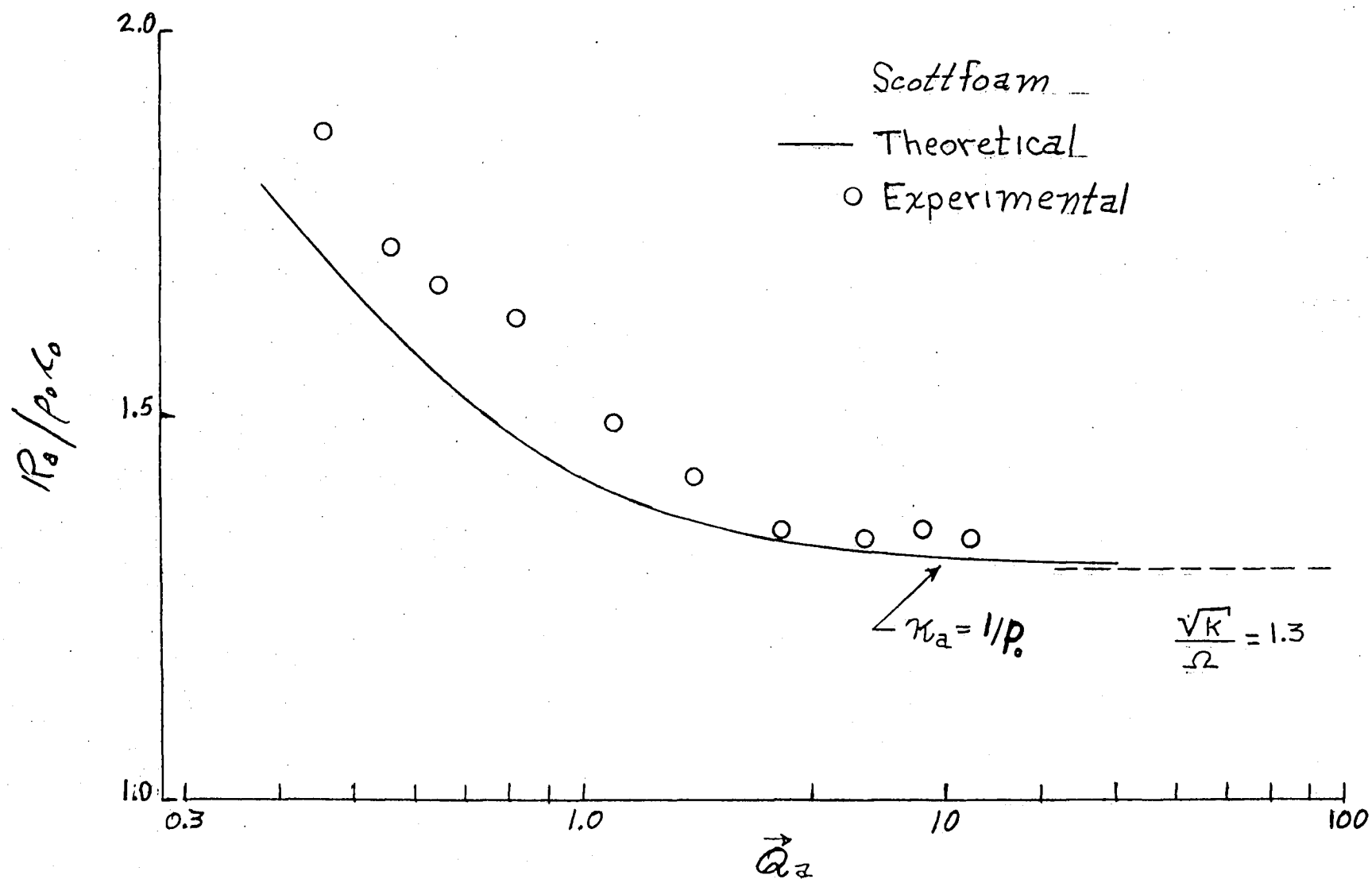


Figure 10.- Comparisons of the normalized acoustic resistance for Scottfoam sample.

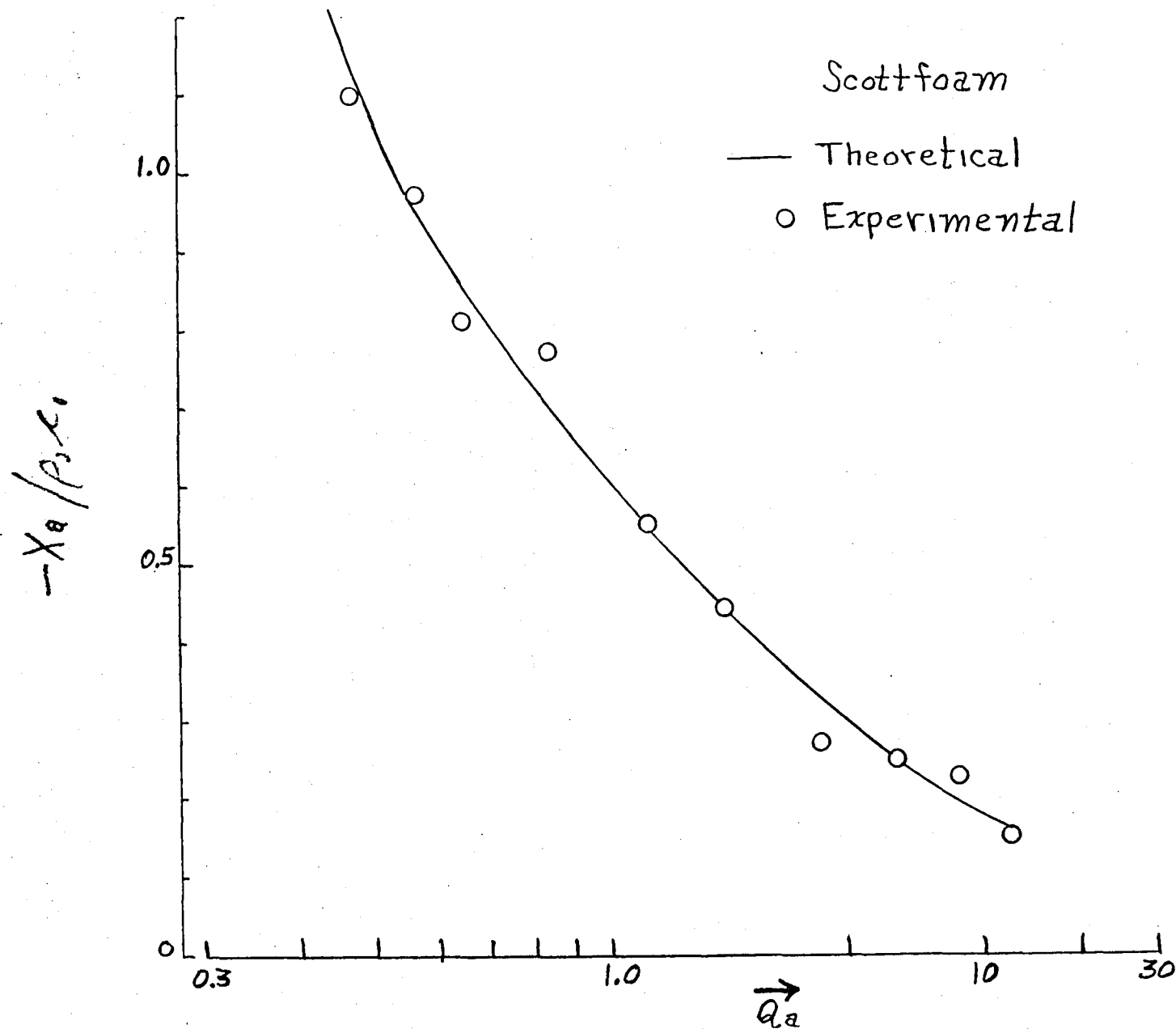


Figure 11.- Comparisons of the normalized acoustic reactance for Scottfoam sample.

Normal Incidence Sound Absorption Coefficient

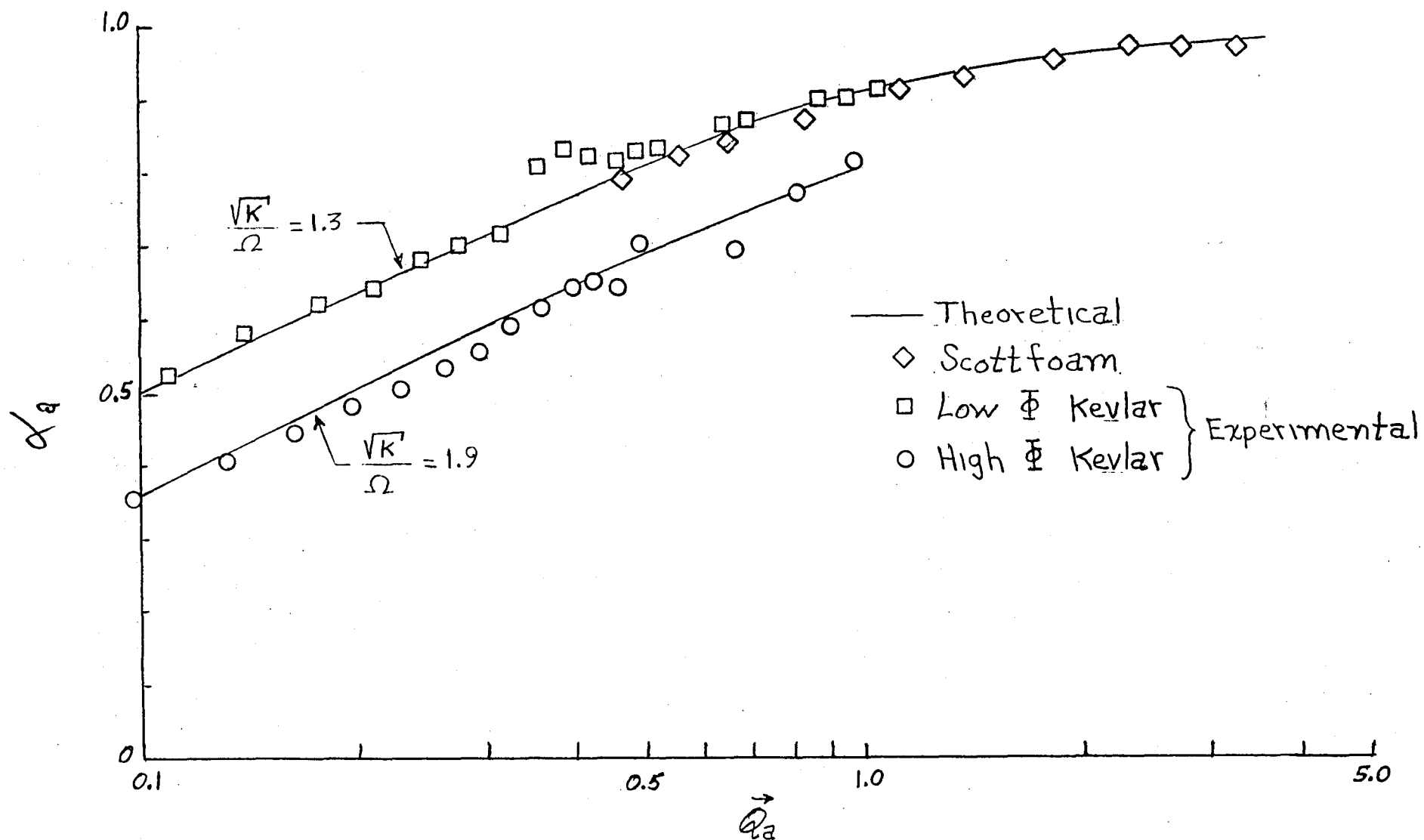


Figure 12.- Comparison of the normal incidence sound absorptive coefficient of Scottfoam, low Φ Kevlar, and high Φ Kevlar samples.

1. Report No. NASA TM-80135		2. Government Accession No.		3. Recipient's Catalog No.	
4. Title and Subtitle ACOUSTICAL PROPERTIES OF HIGHLY POROUS, FLEXIBLE FIBROUS MATERIALS				5. Report Date July 1979	
				6. Performing Organization Code	
7. Author(s) Robert F. Lambert*				8. Performing Organization Report No.	
				10. Work Unit No. 505-03-13-18	
9. Performing Organization Name and Address NASA Langley Research Center Hampton, VA 23665				11. Contract or Grant No.	
				13. Type of Report and Period Covered Technical Memorandum	
12. Sponsoring Agency Name and Address National Aeronautics and Space Administration Washington, D.C. 20546				14. Sponsoring Agency Code	
15. Supplementary Notes *Work performed at Langley Research Center while on leave-of-absence from the University of Minnesota through an assignment under provisions of the Intergovernmental Personnel Act of 1970.					
16. Abstract <p>This report initiates a study of highly porous, fibrous bulk sound absorbing materials with a view toward understanding their properties and performance in a wide variety of applications including liners of flow ducts. It is based on the theory of Zwicker and Kosten, which can be applied to both flexible and stiff structural frames. The basis and criteria for decoupling of acoustic waves in the pores of the frame and compressional waves in the frame structure are established. The equations of motion are recast in a form that illucidates the coupling mechanisms; frictional, inertial, and dilatation.</p> <p>Experimental studies of the normal incidence surface impedance and absorption coefficient of two types of Kevlar 29 and an open-celled foam material are presented, compared, and discussed. Theoretical results can be brought into good agreement with experimental values if the so-called structure factor is selected to provide a fit to the experimental data. A parametric procedure for achieving that fit was established. Both a bulk material quality factor and a high frequency impedance level are required to characterize the real and imaginary part of the surface impedance and absorption coefficient.</p> <p>A new derivation of the concepts of equivalent density and dynamic resistance is presented in the appendix. This work is preliminary to a study of angle of incidence and extended surface reaction effects in bulk duct liner materials.</p> <p>The theory as formulated is relevant to duct acoustics, out-door sound propagation over porous ground cover, and a host of applications in noise control and architectural acoustics.</p>					
17. Key Words (Suggested by Author(s)) Porous Fibrous Materials Wave Coupling Normal Impedance Equivalent Density - Dynamic Resistance			18. Distribution Statement Unclassified - Unlimited Subject Category 71		
19. Security Classif. (of this report) Unclassified		20. Security Classif. (of this page) Unclassified		21. No. of Pages 66	
				22. Price* \$5.25	

